AGU PUBLICATIONS

Reviews of Geophysics

REVIEW ARTICLE
10.1002/2016RG000519

Key Points:
- There are a number of methods used to classify extratropical cyclones that provide insight into their development and impacts
- Evaluation of climate models could benefit from consideration of cyclone types, especially those with stronger diabatic contributions
- Climate change may influence the location, frequency, intensity, and types of cyclones that occur

Correspondence to:
J. L. Catto,
jennifer.catto@monash.edu

Citation:
Catto, J. L. (2016), Extratropical cyclone classification and its use in climate studies, *Rev. Geophys.*, *54*, doi:10.1002/2016RG000519.

Received 19 FEB 2016
Accepted 11 MAY 2016
Accepted article online 20 MAY 2016

Extratropical cyclone classification and its use in climate studies

J. L. Catto[1]

[1] School of Earth, Atmosphere and Environment, Monash University, Clayton, Victoria, Australia

Abstract Extratropical cyclones have long been known to be important for midlatitude weather. It is therefore important that our current state-of-the-art climate models are able to realistically represent these features, in order that we can have confidence in how they are projected to change in a warming climate. Despite the observation that these cyclones are extremely variable in their structure and features, there have, over the years, been numerous attempts to classify or group them. Such classifications can provide insight into the different cloud structures, airflows, and dynamical forcing mechanisms within the different cyclone types. This review collects and details as many classification techniques as possible, and may therefore act as a reference guide to classifications. These classifications offer the opportunity to improve the way extratropical cyclone evaluation in climate models is currently done by giving more insight into the dynamical and physical processes that occur in climate models (rather than just evaluating the mean state over a broad region as is often done). Examples of where these ideas have been used, or could be used, are reviewed. Finally, the potential impacts of future climate changes on extratropical cyclones are detailed. The ways in which the classification techniques could improve our understanding of future changes in extratropical cyclones and their impacts are given.

1. Introduction

Extratropical cyclones (also called midlatitude storms) are a vital component of the global circulation [e.g., *Chang et al.*, 2002], transporting huge amounts of moisture and energy. The passage of these systems is responsible for much of the day-to-day variability of weather in the midlatitudes, with cyclones and fronts bringing up to 90% of the precipitation [*Catto et al.*, 2012; *Hawcroft et al.*, 2012] including extremes (for example, as defined by events above the 99th percentile [*Pfahl and Wernli*, 2012; *Catto and Pfahl*, 2013]) and causing damage associated with strong winds [e.g., *Browning*, 2004; *Leckebusch et al.*, 2006]. It is therefore of great importance that climate models are able to represent these features so that we can have confidence in projections of how these systems may change in a future climate.

Evaluation of extratropical storm tracks is an important part of the process of the Intergovernmental Panel on Climate Change (IPCC), and there has been much recent interest in looking not just at the mean preferred storm locations but also at the structure of extratropical cyclones in climate models and their associated cloud and precipitation features [*Field and Wood*, 2007; *Catto et al.*, 2010; *Govekar et al.*, 2014]. These studies have primarily considered the average properties of a large number of cyclones, without considering their salient features. I would like to propose that there are a number of techniques that have been published, and are available, that could improve the way extratropical cyclone evaluation in climate models is currently done—that is, by utilizing cyclone classification techniques.

Over the years there have been great efforts to study and understand observed extratropical cyclones; how they are initiated, how they grow, their life cycles, and impacts. *Zillman and Price* [1972] stated that, "Inspection of even a few months of daily satellite pictures provides convincing evidence that no two vortices are ever quite the same." Despite this, classifying cyclones according to their similarities has long been considered useful [e.g., *Zillman and Price*, 1972; *Troup and Streten*, 1972] in order to aid in understanding the important mechanisms. There are also physical and dynamical reasons why we would expect cyclones to fit into different classes.

There are certain configurations of the atmospheric flow in the midlatitudes that are expected to force upward motion, thereby inducing cyclogenesis. The subsequent development of the cyclones is also sensitive to the

background flow [e.g., *Hoskins and West*, 1979; *Davies et al.*, 1991; *Thorncroft et al.*, 1993; *Pinto et al.*, 2014]. As a result of so many processes to consider, the classification of extratropical cyclones has been approached in many different ways. Examples of these include simple conceptual models, idealized modeling, cloud features, forcing mechanisms, synoptic and dynamic features, and impacts.

With so many ways of grouping and classifying cyclones, the first goal of this review paper is to collect and detail as many classification techniques as possible: how the classification is done, what the main features of the different classes are, and how they have been applied in the past. An attempt is made to link the different classification results together by identifying similarities in the observed classes. This review can then serve as a reference manual for extratropical cyclone classification techniques (see section 3).

The second goal, covered in section 4, is to review what has been done in relation to the evaluation of extratropical cyclones in climate models. The most recent IPCC report [*Flato et al.*, 2013] included a section on model evaluation of the extratropical storm tracks (either defined as a maximum in Eulerian measures such as eddy kinetic energy, or in Lagrangian cyclone tracking track densities). The focus here will therefore be on instances in which classification techniques have been used and then identifying where they could be further applied. These techniques can offer a more detailed evaluation of cyclones compared to just considering the average structure over many, often quite different, composited cyclones. The classifications can also offer insight into the dynamical and physical processes that occur in climate models.

With a changing climate it seems likely that not all cyclones will be affected in the same way. Making use of classifications may help to diagnose and understand projected changes in extratropical cyclones. There are only very few studies that have made use of such techniques when looking at future changes. Section 5 will therefore primarily focus on projected changes in extratropical cyclones and will identify other climatic factors that could influence how the many different classes of cyclones may change. Finally, a critical analysis of which techniques may be useful in climate model evaluation and investigation of future changes, and how this field of study can be moved forward by using the newest data available is given in section 6.

2. Introduction to Baroclinic Instability and Potential Vorticity Thinking

In almost all discussions on extratropical cyclones, reference will be made to baroclinic instability or baroclinicity. This is the primary mechanism by which extratropical cyclones develop and so it deserves some attention in a review such as this. Another important concept is the so-called *PV thinking* [*Hoskins et al.*, 1985], and a brief introduction is given here. Readers familiar with these concepts may wish to skip to section 3.

Potential vorticity (PV) is a conserved quantity for adiabatic, frictionless flow. It is a measure of the circulation of a fluid parcel between two isentropic surfaces and depends on the absolute vorticity and the static stability (or stratification) of the atmosphere. PV is typically higher in the stratosphere and lower in the troposphere and the tropopause is often defined as the level in the atmosphere above which the PV is greater than 2 PVU (potential vorticity units; 1 PVU = $10-6$ K kg^{-1} m^2 s^{-1}) in the Northern Hemisphere (NH) and less than -2 PVU in the Southern Hemisphere (SH). Above this level the gradient of PV increases markedly.

2.1. Baroclinic Instability

Due to the differential heating of Earth by the Sun, there is a strong meridional temperature gradient in the midlatitudes. Through thermal wind balance, this temperature gradient creates a vertical shear of zonal wind, and flow that is unstable to small perturbations. This is a type of wave instability that grows by converting available potential energy into kinetic energy. One way to think of baroclinic growth is the interaction of two waves (counterpropagating Rossby waves)—one at the surface and one near the tropopause [e.g., *Hoskins et al.*, 1985]. Figure 1 shows a schematic diagram of the concept of baroclinic interaction. Consider a mean state in which there is a positive equator-to-pole potential vorticity (PV) gradient at upper levels and a negative equator-to-pole temperature gradient at the surface. An upper level trough (i.e., a cyclonic PV anomaly—positive in the NH and negative in the SH), through action at a distance, induces a cyclonic circulation at the surface. This produces positive (and negative) anomalies of temperature at the surface that also have associated cyclonic (and anticyclonic) circulations. The waves at each level act to enhance the amplitude of each other and a small perturbation can grow. The upper level wave propagates westward relative to the mean flow, while the low-level wave propagates eastward relative to the mean flow. The vertical shear of zonal wind means that there is the possibility of the counterpropagating Rossby waves phase locking, hence producing an unstable growth mechanism.

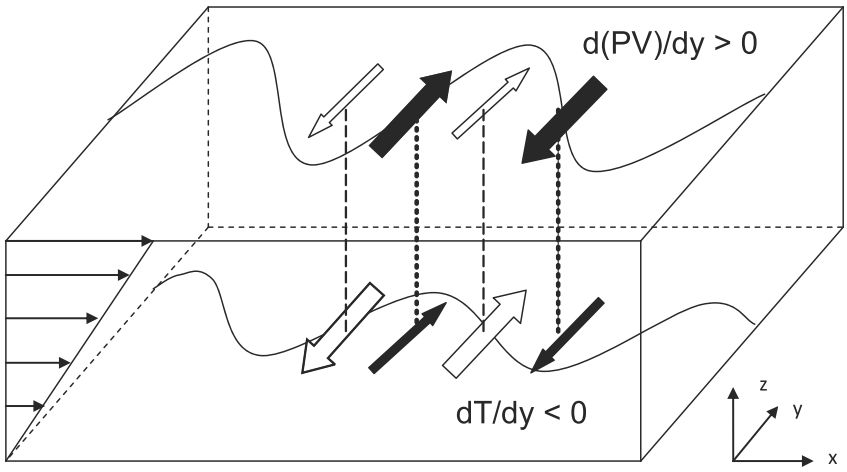

Figure 1. Schematic diagram of baroclinic instability in the Northern Hemisphere, with waves on the surface and the upper boundary. There is constant wind shear with height, indicated by the thin black arrows on the left of the diagram. The large black filled arrows indicate the circulation on the upper level due to the PV anomaly, the small black filled arrows indicate the induced flow at the surface. The large nonfilled arrows indicate the circulation due to the surface temperature anomaly, while the small nonfilled arrows indicate the circulation induced at the upper level.

Some early mathematical descriptions of baroclinic instability include the Eady Model [*Eady*, 1949] and the Charney Model [*Charney*, 1947]. The maximum growth rate from the Eady Model is often used as a diagnostic of the baroclinicity of the atmosphere [e.g., *Lindzen and Farrell*, 1980]. This measure is a good indicator of the possibility of extratropical cyclone development [*Hoskins and Valdes*, 1990] and is a necessary factor in the development of some types of cyclones, which will be discussed throughout the review.

2.2. PV Thinking

The description of baroclinic instability given above assumes growth from small perturbations. However, in the real atmosphere, there are usually finite amplitude anomalies at either upper or lower levels. *Hoskins et al.* [1985] developed the concept of "PV thinking" in order to understand atmospheric circulation through interactions of different anomalous features. Due to PV being a conserved quantity, its rate of change can be predicted by advection. Any further changes can be attributed to the creation or destruction of PV by diabatic processes (friction, latent heating, and radiative heating).

PV can also be inverted (assuming some appropriate balance conditions) to give the dynamic (winds and geopotential) and thermodynamic (potential temperature) state of the atmosphere [*Davis and Emanuel*, 1991]. Figure 2 shows the potential temperature and circulation field associated with upper level cyclonic PV anomalies. When the tropopause is lowered, bringing a positive PV anomaly (negative in the SH), potential temperature contours bend up toward the anomaly, giving a cold anomaly, and a cyclonic circulation is induced. The effects of the circulation spread to the surface, thereby inducing surface extratropical cyclogenesis.

3. Different Approaches to Classification

In this section the many different ways of classifying extratropical cyclones are detailed, including the techniques, the features of the classes, and how they may have been applied. This provides a basis for sections 4 and 5, in which the (potential) applications of the classifications are discussed.

3.1. Simple Conceptual Models and Life Cycle Characteristics

3.1.1. The Development of Conceptual Models

Some of the early work on understanding the passage of extratropical cyclones was developed in Norway by the group of Vilhelm Bjerknes. They developed a conceptual understanding of such cyclones through the use of surface-based weather observations and eventually their meteorological teachings became known as the *Bergen School of Meteorology*. The particular conceptual model they developed to describe cyclone genesis and development [*Bjerknes and Solberg*, 1922] is now known as the *Norwegian model* in their honor (see Figure 3a). This model describes the passage of families of cyclones developing along a sharp meridional

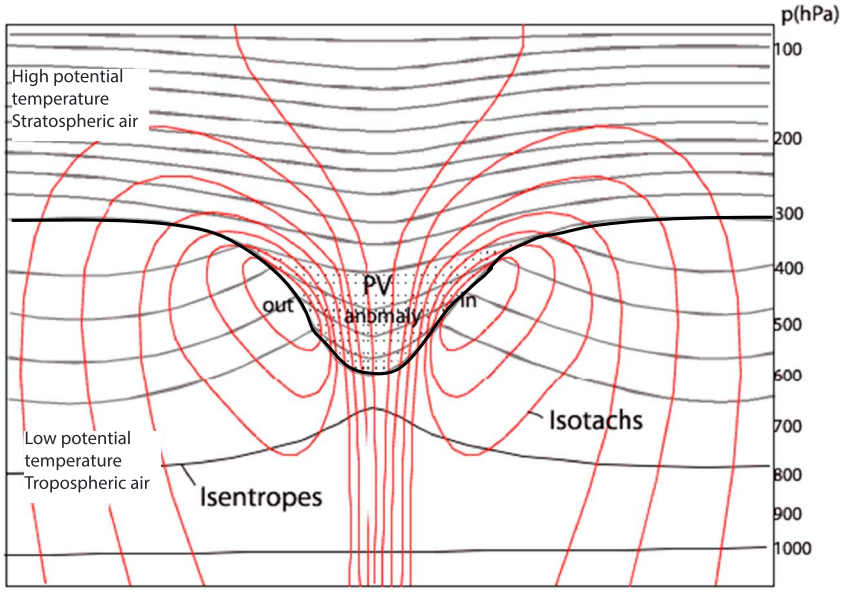

Figure 2. Vertical structure of potential temperature and wind anomalies associated with a cyclonic isentropic PV anomaly (a lowered tropopause; shown as the stippled region) for the Northern Hemisphere. The thick black line represents the tropopause. Following *Hoskins et al.* [1985].

temperature gradient known as the polar front (Figure 3a, I). A kink in the polar front develops into a low pressure system with warm and cold fronts and associated rainfall, and a warm sector (Figure 3a, II–III). As the cyclone continues through its life cycle, the warm sector narrows and the fronts become occluded as the cyclone deepens (Figure 3a, IV). Eventually the occlusion grows and the warm sector no longer remains, with the original version of the model showing a pinching-off of some warm air near the center of the cyclone (not shown in Figure 3a). The trailing cold front is then considered the polar front ready for the next cyclone development.

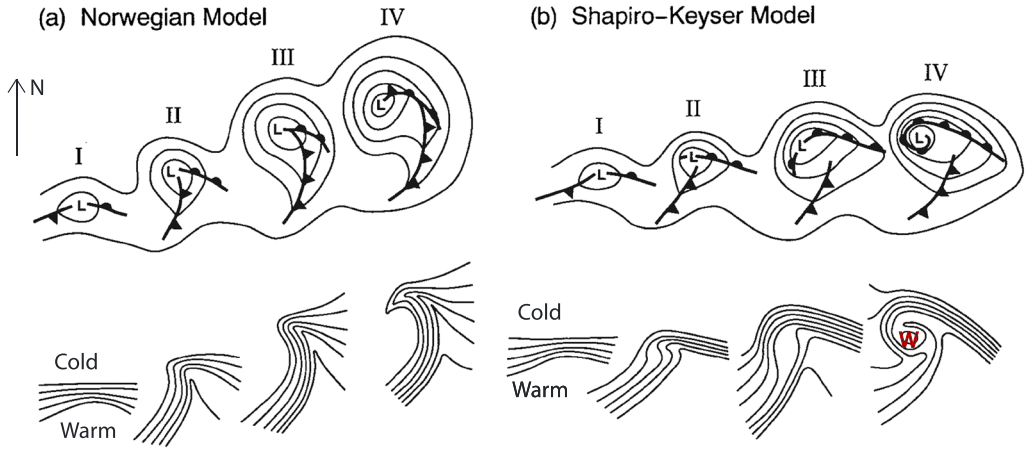

Figure 3. Conceptual models of cyclone evolution showing (top) lower tropospheric (e.g., 850hPa) geopotential height and fronts, and (bottom) lower tropospheric potential temperature (going from cold on the north side to warm on the south side). (a) Norwegian cyclone model: (I) incipient frontal cyclone, (II and III) narrowing warm sector, and (IV) occlusion; (b) Shapiro-Keyser cyclone model: (I) incipient frontal cyclone, (II) frontal fracture, (III) frontal T-bone and bent-back front, and (IV) frontal T-bone and warm seclusion. Figure 3b is adapted from *Shapiro and Keyser* [1990] (their Figure 10.27) to enhance the zonal elongation of the cyclone and fronts and to reflect the continued existence of the frontal T-bone in stage IV. The stages in the respective cyclone evolutions are separated by approximately 6–24h and the frontal symbols are conventional. The characteristic scale of the cyclones based on the distance from the geopotential height minimum, denoted by *L*, to the outermost geopotential height contour in stage IV is 1000 km. (From *Schultz et al.* [1998], ©American Meteorological Society, reprinted with permission.)

The ability to forecast the weather motivated a lot of the early conceptual models of cyclogenesis and the polar front theory, including the Norwegian model (see *Uccellini et al.* [1999], for a historical overview of the forecasting of extratropical cyclones). The Norwegian model of cyclone life cycles has, therefore, been widely used in forecasting and also in teaching synoptic meteorology. Nevertheless, the occlusion process with a narrowing warm sector (a process that has often been described as the cold front "catching up" to the warm front, but more recently—and accurately—being described as the fronts "wrapping up" [*Schultz and Vaughan*, 2011], has not been found to be universally applicable.

A large number of idealized modeling studies aimed to simulate the life cycles of baroclinic waves or cyclones using varying levels of complexity. These simulations did not exhibit the same features as the Norwegian life cycle model. For example, *Hoskins and West* [1979] found no occluded fronts developed, while *Polavarapu and Peltier* [1990] found that the occlusion developed as the warm air turned cyclonically and was cut off from the main warm air mass. Other modeling studies also found many differences between their simulations and the Norwegian model [e.g., *Hoskins*, 1976, 1981; *Keyser et al.*, 1989]. More realistic simulations of real cyclones also produced cyclones with features different from the Norwegian model [*Shapiro and Keyser*, 1990].

In the late 1980s there were a number of intensive observing campaigns whose focus was on understanding rapid cyclogenesis, including the Fronts and Atlantic Storm-Track EXperiment (FASTEX) [*Joly et al.*, 1997, 1999] and the Experiment on Rapidly Intensifying Cyclones over the Atlantic (ERICA) [*Hadlock and Kreitzberg*, 1988]. The life cycle of one the cyclones observed during ERICA was described in detail by *Neiman and Shapiro* [1993] and *Neiman et al.* [1993]. Using these observations and observations from other field-observing programs, *Shapiro and Keyser* [1990] proposed a new conceptual model of the life cycle of extratropical cyclones. In this life cycle, the incipient cyclone starts in much the same way as the Norwegian model, on a broad frontal region (Figure 3b, I). In the next phase, the cold and warm front separate at the cyclone center (fracture) and become narrower and stronger (Figure 3b, II). The cold front moves across the cyclone, while the warm front extends rearward, forming a characteristic "T-bone" structure (Figure 3b, III). In the final stage of the life cycle, relatively warm air becomes wrapped up in the center of the cyclone forming a warm seclusion (Figure 3b, IV). It should be noted that this warm seclusion is not the result of warm sector air being pinched off, as is suggested in the model of *Bjerknes and Solberg* [1922], but rather the wrapping up of the warm air in the center of the cyclone.

Later work has suggested that actually there may be some cyclones that more closely resemble the Shapiro-Keyser model, and some that more closely resemble the Norwegian model. *Schultz et al.* [1998] suggested that cyclones occurring in diffluent flow develop in a way that is similar to the Norwegian model, whereby the cold front is pulled in a more meridional direction and is stronger than the warm front. On the other hand, cyclones look more like the Shapiro-Keyser model when they occur in confluent flow, with the cold front being more zonally elongated, and the warm front being stronger (a feature that was evident in the cyclone of *Neiman and Shapiro* [1993]).

3.1.2. Idealized Modeling

Idealized modeling studies have proved an extremely useful tool in the development of theories regarding the evolution of extratropical cyclones and their associated fronts [e.g., *Hoskins and West*, 1979; *Simmons and Hoskins*, 1980; *Emanuel et al.*, 1987; *Davies et al.*, 1991; *Thorncroft et al.*, 1993; *Fantini*, 2004], as well as their impacts [*Polvani and Esler*, 2007; *Sinclair et al.*, 2008]. *Thorncroft et al.* [1993] simulated two different baroclinic life cycles, which differed only in the amount of cyclonic shear in the initialization [e.g., *Simmons and Hoskins*, 1980]. These life cycles exhibited quite different developments over their lifetimes. The first (LC1) exhibited anticyclonic (or equatorward of the jet) Rossby wave breaking (RWB) with elongated upper level PV streamers eventually leading to a cutoff of cyclonic PV. This upper level PV anomaly then interacted with the low-level frontal structure to eventually form a secondary cyclone (see section 3.4). The second life cycle (LC2), which started with more cyclonic shear, exhibited cyclonic RWB (with the features wrapping up poleward of the jet), resulting in much broader, more meridionally confined PV anomalies and larger surface cyclones. These two contrasting life cycles have been extremely useful in many studies of real-world scenarios, for example, in understanding blocking and how this relates to cyclogenesis at the surface [*Gómara et al.*, 2014; *Michel et al.*, 2012; *Barnes and Hartmann*, 2012], and for describing flow regimes at different times [e.g., *Sodemann and Stohl*, 2013]. Methods to objectively detect RWB events [e.g., *Wernli and Sprenger*, 2007; *Martius et al.*, 2007, 2008; *Masato et al.*, 2013a] and define them as anticyclonic or cyclonic and, therefore, LC1 or LC2 may be a useful tool in the evaluation of climate models [*Béguin et al.*, 2013; *Masato et al.*, 2013b] and their ability to represent the large-scale and smaller-scale features of extratropical cyclogenesis.

Many of the studies described above focused on relatively small regions, such as the North Atlantic, due to the requirement for observations to validate the theory and modeling. It is possible that certain features and life cycles may be more evident in some regions than others, and there may be a spatial distribution to the type of life cycle that is most common. *Chang and Song* [2006] identified differences in cyclone characteristics between the North Atlantic and North Pacific. Such differences may be associated with the differing orientations of the jet stream in these regions or with the shape of the bordering landmasses [e.g., *Brayshaw et al.*, 2009]. The development of higher-resolution, observationally constrained data sets (e.g., reanalysis data sets), particularly including a lot of remote sensing observations, provides an opportunity to investigate this in more detail. Features that could be used to identify the two different conceptual life cycles could be the warm seclusion, the relative strength and orientation of the warm and cold fronts, and the frontolysis evident in the frontal fracture zone. The ideas put forward by *Schultz et al.* [1998] could then be tested on a large scale, and the ability of relatively low-resolution climate models to simulate these features examined.

3.1.3. Explosive Cyclones

One particular life cycle characteristic that has been used to separate out certain cyclones is their rapid deepening or "explosive cyclogenesis." The widely accepted way to define such a "bomb" is that its central pressure must fall by at least 1 bergeron (defined as $24(\sin\phi/\sin 60°)$ hPa in 24 h [*Sanders and Gyakum*, 1980], where ϕ is the latitude of the cyclone, following the work of Tor Bergeron). In regions where there is a strong meridional gradient of climatological mean sea level pressure, consideration of the central pressure change relative to the climatological mean sea level pressure is more meaningful [*Lim and Simmonds*, 2002]. Such cyclones can have large impacts due to their precipitation, storm surge, or strong winds [e.g., *Sanders and Gyakum*, 1980; *Fink et al.*, 2009; *Liberato et al.*, 2011] and can be difficult to forecast ([e.g., *Sanders*, 1987; *Gyakum et al.*, 1996]). *Sanders and Gyakum* [1980] developed a climatology of such cyclones in the NH, finding the largest frequencies of occurrence in the western North Atlantic close to the coast of North America, over the Kuroshio current region to the east of Japan, and in the mid-Pacific (based on three cold seasons). This was further confirmed by the updated climatologies of *Roebber* [1984], *Chen et al.* [1992], and by a comparative study of the NH and SH using objective cyclone tracking by *Lim and Simmonds* [2002]. In the SH the regions of occurrence of explosive cyclogenesis are not quite so constrained as in the NH, consistent with the patterns of the overall storm tracks. Nevertheless, there are maxima in winter in the Southern Ocean south of Australia, to the east of Australia, in the south central Pacific, and to the east of the South American continent.

The correspondence of the preferred locations for explosive cyclogenesis and strong baroclinicity points toward the importance of baroclinic instability for this phenomenon [*Sanders and Gyakum*, 1980; *Wang and Rogers*, 2001; *Lim and Simmonds*, 2002]. As we shall see for other classes of cyclones, this is not the only important ingredient. Other factors involved in explosive cyclogenesis are upper level forcing, air-sea interactions, and diabatic heating—these vary in importance between cyclones and depending on their location. For example,

1. Upper level forcing may be associated with upper level PV anomalies [e.g., *Elsberry and Kirchoffer*, 1988; *Wang and Rogers*, 2001; *Dacre and Gray*, 2013; *Kouroutzoglou et al.*, 2015], potentially caused by either cyclonic or anticyclonic Rossby wave breaking [*Gómara et al.*, 2014] and this seems to be more important in the east Atlantic than the west Atlantic [*Wang and Rogers*, 2001; *Dacre and Gray*, 2013].
2. Air-sea interaction involves the flux of energy from the ocean to the atmosphere, resulting in heating and moistening of the atmosphere and reduced stability, which is important prior to and during the explosive development [*Davis and Emanuel*, 1988; *Kuo et al.*, 1991; *Reed et al.*, 1993]. Moisture from the ocean may be transported onshore, contributing to latent heating in the cyclones [*Brennan and Lackmann*, 2005] and it may be evaporated by drier airstreams within the cyclones, leading to enhanced latent heat release in the warm conveyor belt region of the cyclone [*Booth et al.*, 2012; *Hirata et al.*, 2015].
3. Latent heat release (diabatic heating) can be very important in the generation and/or development of explosive cyclones [*Anthes et al.*, 1983; *Manobianco*, 1989; *Lim and Simmonds*, 2002; *Heo et al.*, 2015; *Kouroutzoglou et al.*, 2015]. *Heo et al.* [2015] find that the latent heat released in an explosive cyclone could account for around half of the intensification seen during the initial phase of cyclone development. However, *Manobianco* [1989] found that the latent heat release from convection was more important during the latter stages of cyclone development.

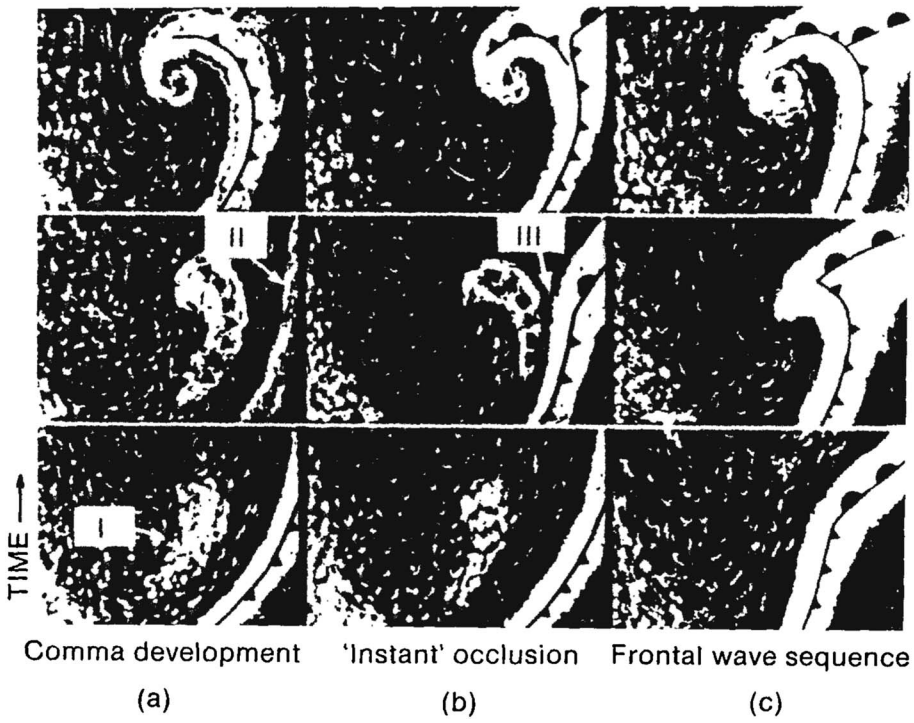

Figure 4. Schematic depiction of three basic sequences of vortex development evident in satellite imagery. See section 3.2 for description. White dots represent regions of convection, solid white areas represent stratiform cloud. Label I shows enhanced convection, label II shows the decaying cloud band, and label III shows the convective mass and cloud band merging. (From *Browning* [1990], ©American Meteorological Society, reprinted with permission.)

Recently, *Fink et al.* [2012] decomposed the diabatic contributions to a number of explosively developing cyclones in the northeast Atlantic. In some of the cyclones considered, diabatic heating played a greater role in cyclone development than temperature advection, whereas in others, the diabatic processes were less important. Such a tool could be used to objectively classify cyclones in reanalysis data and subsequently evaluate them in climate models.

3.2. Satellite Classification

In the 1960s, satellites began to be used for meteorological purposes and it became possible to view extratropical cyclones from above by their distinctive cloud signatures. From these cloud signatures, upper level flow features can be inferred and, when combined with analysis data, are a powerful tool for understanding extratropical cyclogenesis [e.g., *Zillman and Price*, 1972; *Browning*, 1990; *Evans et al.*, 1994]. This is especially useful for deep cyclones (those with low central pressure), since cloud features become more distinct in deeper cyclones (when considering cyclones at any point in their life cycle) [*Field and Wood*, 2007]. Satellite classification has mostly been used to classify the cyclogenesis as an aid to forecasting [e.g., *Zillman and Price*, 1972; *Reed*, 1979; *Reed and Blier*, 1986a, 1986b; *Evans et al.*, 1994; *Young*, 1993]. Others have used satellite data to look at different cyclone life cycles [e.g., *Troup and Streten*, 1972] or relate cloud features to cyclone intensities [*Junker and Haller*, 1980].

One of the first studies to classify cyclogenesis from satellite data was that of *Zillman and Price* [1972]. They classified a number of cyclones in the SH according to the cloud configurations viewed in photos from the "Automatic Picture Transmission" from weather satellites. Three configurations were identified over the Southern Ocean and later shown by *Browning and Hill* [1985] and *Browning* [1990] to be applicable to the NH. The NH version of the schematic representation of the three classes is shown in Figure 4. The three classes from *Zillman and Price* [1972] are as follows:

1. The comma development. This occurs in a region of cold air and has also been referred to as cold-air cyclogenesis. A cloud cluster associated with a cyclonic vortex develops far from the main polar front (and the typical warm conveyor belt, see next section).

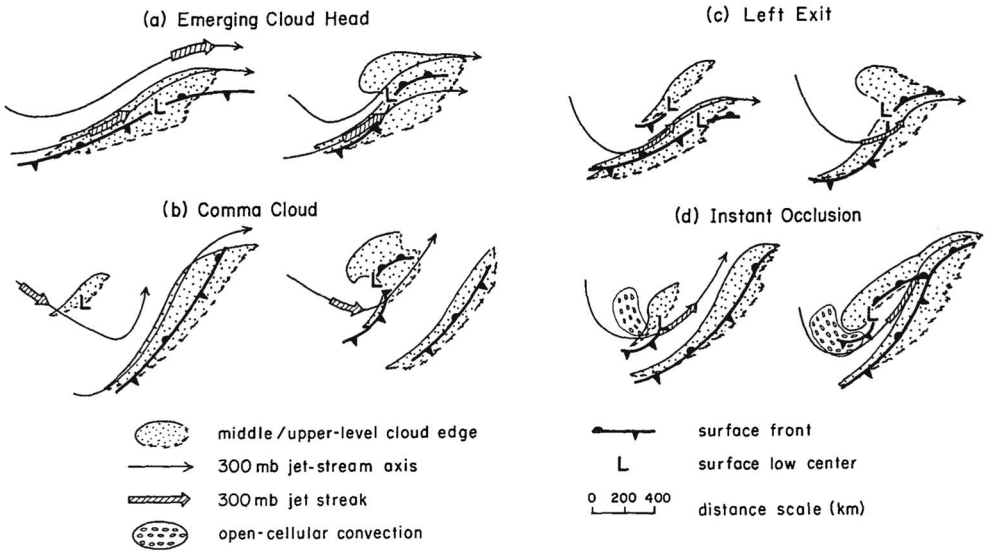

Figure 5. Schematic representation of the four types of cyclogenesis proposed in *Evans et al.* [1994]: (a) The emerging cloud head; (b) the comma cloud; (c) the left exit; and (d) the instant occlusion. Temporal separation between early (left) and later (right) stages of evolution is approximately 12–24 h. Frontal symbols are conventional; remaining symbols are defined in the legend. (From *Evans et al.* [1994], ©American Meteorological Society, reprinted with permission.)

2. The instant occlusion. In this class the cloud cluster (also referred to as a baroclinic leaf) catches up to the polar front cloud band and interacts with the warm conveyor belt (WCB).
3. The frontal-wave sequence. This is identified as the development of a cloud head as the WCB rises over the surface warm front [*Browning*, 1990].

A number of other schemes of extratropical cyclone classification using satellite imagery were developed [e.g., *Mullen*, 1983; *Browning and Hill*, 1985; *Young*, 1993, 1996]; however, in their thorough overview, *Evans et al.* [1994] found that each of the classes identified in these studies could be related to the three classes proposed by *Zillman and Price* [1972] (apart from one case from *Young* [1993, 1996]).

Evans et al. [1994] developed a new classification scheme for cyclogenesis, focusing on rapid deepening events in the western North Atlantic. They used satellite data to develop their classifications but combined these with analysis data to provide information about the upper level flow and the surface cyclone development. The four classes from *Evans et al.* [1994] are shown in Figure 5 and a description is given below.

1. Emerging Cloud Head (Figure 5a). In this class, the cyclogenesis occurs along the surface polar front and is seen when a typical anticyclonic cloud head becomes visible poleward of the main polar front cloud band. The upper level flow is typically fairly zonal and occurs downstream of a confluent trough in the left jet exit region.
2. Comma Cloud Development (Figure 5b). This occurs when cyclogenesis occurs upstream of and on the cold-air side of the polar front cloud band and there is no interaction between the two, as for the *Zillman and Price* [1972] class of the same name. The surface cyclone develops underneath the left exit region of a jet streak.
3. Left Exit (Figure 5c). This class can be identified by the merger of two cloud features: the baroclinic leaf and the polar front cloud band. Like the comma cloud development, left exit development occurs upstream of the polar front cloud band and associated with a deep upper level trough and diffluent flow.
4. Instant Occlusion (Figure 5d). This class of cyclogenesis also involves the merger of a cloud cluster with the polar front cloud band, but deepening occurs in the entrance region of a jet streak, i.e., confluent flow. In this case, the cloud cluster exhibits more convective cloud characteristics compared to the left exit case.

The left exit class and the instant occlusion of *Evans et al.* [1994] are most similar to the instant occlusion of *Zillman and Price* [1972] and *Browning and Hill* [1985]; however, the two classes of *Evans et al.* [1994] vary in their upper level flow configuration (i.e., left jet exit versus jet entrance) and therefore the resulting orientation and structure of the clouds. The emerging cloud head resembles the frontal-wave sequence, and the comma cloud resembles the comma development.

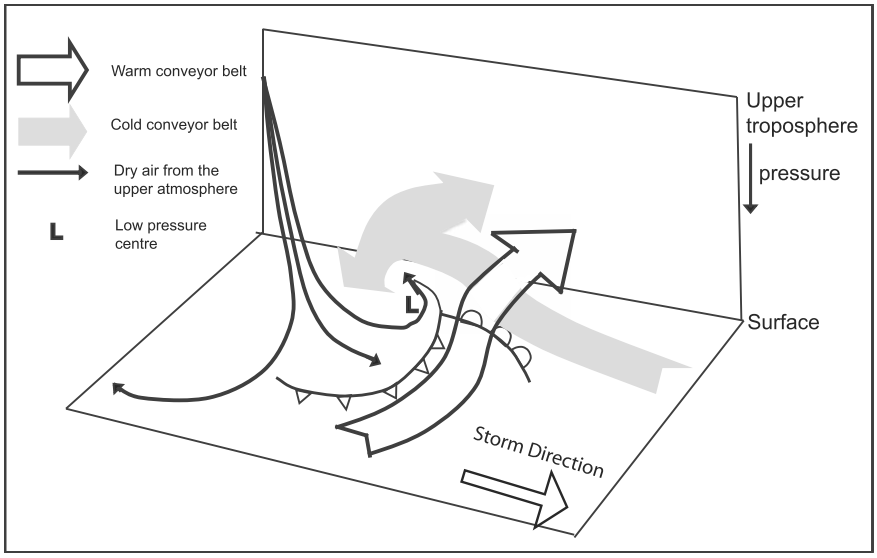

Figure 6. Schematic showing warm conveyor belt (WCB), cold conveyor belt (CCB), and dry intrusion (DI) (adapted from *Browning* [1997]). (From *Catto et al.* [2010], ©American Meteorological Society, reprinted with permission.)

3.3. Airstream Analysis

A number of studies attempted to explain the cloud features of extratropical cyclones using the ideas of cyclone-relative airflows [*Harrold*, 1973; *Carlson*, 1980; *Browning*, 1990], initially from a bulk air mass perspective using isentropic flow maps. There are three main airflows that can often be identified within an extratropical cyclone; the warm conveyor belt (WCB), the cold conveyor belt (CCB), and the dry intrusion (DI), shown schematically in Figure 6. The WCB is a stream of warm moist air typically traveling poleward parallel to the cold front [*Harrold*, 1973; *Carlson*, 1980]. The warm air rises over the warm front and eventually turns anticyclonically at upper levels. This airstream is the most important for producing precipitation within extratropical cyclones [*Browning*, 1990]. *Browning* [1986] identified two different types of WCB; a forward sloping WCB associated with a wide area of moderate-to-heavy precipitation; and a rearward sloping WCB associated with a narrow region of very heavy precipitation along the cold front, and behind it a larger region of light precipitation. The CCB travels rearward relative to the cyclone propagation, at lower levels undercutting the WCB, with the main path being cyclonic around the cyclone center, but partly anticyclonic as it ascends into the cloud head [*Schultz*, 2001]. The DI is a flow of colder, drier air descending behind the cyclone. This tends to fan out at lower levels either anticyclonically or cyclonically [*Thorncroft et al.*, 1993], generating the distinctive dry slot along the rearward side of the cold front seen in satellite images. The cyclonic turning dry air can overrun the cold front, generating instability and potential for severe convection [*Browning*, 1990].

Lagrangian parcel trajectory analysis has proved a valuable tool in further investigating WCBs [e.g., *Wernli and Davies*, 1997; *Wernli*, 1997], which are often defined as trajectories ascending by some threshold within a certain time period (e.g., 600 hPa in 2 days [*Madonna et al.*, 2014a]). This definition identifies features that are smaller than what might be determined from isentropic flow maps. Trajectory analysis has shown that WCBs bring anomalously anticyclonic PV to upper levels—due to the condensational heating that occurs during the parcel ascent—contributing to downstream development [*Joos and Wernli*, 2012; *Schemm et al.*, 2013; *Madonna et al.*, 2014a], and they are often associated with very heavy precipitation events [*Pfahl et al.*, 2014; *Catto et al.*, 2015a]. Objective climatologies of WCBs have been produced from reanalysis data [*Eckhardt et al.*, 2004; *Madonna et al.*, 2014a] and the relationship between the WCB and CCB investigated in idealized simulations of cyclones [*Schemm and Wernli*, 2014]. Additionally, the cloud structures associated with the airflows can be identified using satellite data [e.g., *Naud et al.*, 2012; *Govekar et al.*, 2011].

Combining these climatologies with objective methods of cyclone detection and tracking and front identification [e.g., *Catto et al.*, 2015a] gives potential to classify cyclones according to the relative strength of the WCB, CCB, and DI. These characteristics would also manifest themselves in the cloud features. Linked to this, a combination of trajectory analysis, satellite cloud information, and objective frontal climatologies [e.g., *Berry et al.*, 2011] could be used to objectively identify the forward sloping and rearward sloping WCBs that

Catto et al. [2015a] suggested may preferentially occur in different geographical regions. Since these typically lead to quite different cloud structures and precipitation, the simulation of the correct relative frequency of such systems is vital for understanding future precipitation changes, and cloud impacts on circulation. One limitation of current archived climate model output, for this sort of analysis, is the temporal and vertical resolution required for the trajectory analysis, but this could be performed by individual modeling centers on their own models.

3.4. Synoptic-Dynamic Classification

3.4.1. Upper Level Versus Lower Level Forcing

The conceptual model of cyclogenesis and cyclone life cycles following the work of the Bergen School suggests that synoptic cyclones are generated in the baroclinic environment of the polar front. A second proposed mechanism for cyclogenesis was tested by *Petterssen et al.* [1955] as the hypothesis that "cyclonic development at sea level occurs when and where an area of positive vorticity advection in the upper troposphere becomes superimposed upon a frontal zone at sea level." *Petterssen and Smebye* [1971] looked in more detail at these two mechanisms and developed a classification of them based on the relative contribution of upper level and lower level forcing in the development of the cyclones. The study of *Deveson et al.* [2002] attempted to quantify the upper level and lower level forcing present through the life cycle in a number of cyclones observed during FASTEX [*Joly et al.*, 1997, 1999]. This was done by using a height-attributable version of the quasi-geostrophic omega equation — this determines the forcing of ascent and descent at 700 hPa attributable to both thermal advection at low levels (L) and vorticity advection at upper levels (U). The ratio of this forcing (U/L) is used as a measure of the relative forcing, and the horizontal distance between the maximum upper level and lower level forcing is referred to as the vertical tilt. As well as the two types identified by *Petterssen and Smebye* [1971], *Deveson et al.* [2002] also identified a third type. The three types are as follows:

1. Type A. These cyclones form in a baroclinic zone with a surface frontal feature. In the classification of *Petterssen and Smebye* [1971] they specified that there was no preexisting upper level trough; however, *Deveson et al.* [2002] suggested this was due to deficiencies in the upper level analysis — weak upper level features could not so easily be identified. Thermal advection at low levels is large and vorticity advection at upper levels is small, and the U/L ratio found in *Deveson et al.* [2002] is close to 1. Type A cyclones tend to have a constant vertical tilt (i.e., the horizontal distance between the upper level and lower level forcing remains constant) during their development, indicating phase locking of the levels, akin to the baroclinic instability mechanism shown in Figure 1. *Gray and Dacre* [2006] defined slightly different thresholds of the U/L ratio to identify the three types of cyclone and found that Type A represents 30% of all cyclones in the North Atlantic region, with 60% of this type found to deepen. *Dacre and Gray* [2009] only considered the developing cyclones and found that in the west Atlantic and east Atlantic, Type A cyclones represented 24% and 11% of cyclones, respectively. (The studies of *Dacre and Gray* [2009] and *Gray and Dacre* [2006] used only cyclones identified as frontal waves using the database from *Hewson* [1998.])
2. Type B. These cyclones occur when a preexisting upper level trough moves over a region of warm advection, giving high values of vorticity advection at upper levels. The thermal advection at low levels is small to start with and increases as the low-level circulation is induced. The average value of U/L for type B cyclones is between 1.2 and 3.0 [*Deveson et al.*, 2002]. Due to the progression of the upper level trough, the tilt between the surface low and the upper level trough decreases as the cyclone develops, giving a negative correlation over the cyclone life cycle between tilt and cyclone intensity. *Deveson et al.* [2002] called this type "frontal-wave cyclone," and all Type Bs considered in *Deveson et al.* [2002] were found to be second-generation waves on fronts (i.e., secondary frontal waves) [*Parker*, 1998] by *Joly et al.* [1999]. Type B cyclones are the most prevalent of the three types in the North Atlantic making up 38% of cyclones identified by *Gray and Dacre* [2006]; 56% of these develop. Of developing cyclones, type B represents 51% and 50% in the west and east Atlantic, respectively [*Dacre and Gray*, 2009].
3. Type C. These cyclones were initially identified by *Deveson et al.* [2002] as cyclones that had very strong upper level forcing, but a weak temporal correlation between the tilt and the cyclone intensity. These represented 32% of all cyclones identified in *Gray and Dacre* [2006], but only 31% of these subsequently developed. Of the developing cyclones, Type C were found to be more prevalent in the east Atlantic than in the west Atlantic region [*Dacre and Gray*, 2009]. Explosive development can occur once the upper and lower levels become coupled. *Plant et al.* [2003] performed a detailed study on some postulated Type C cyclones and found three important aspects: "(i) the crucial role of strong midlevel latent heating; (ii) the absence of significant surface thermal anomalies; and (iii) interactions of the diabatic and upper level anomalies

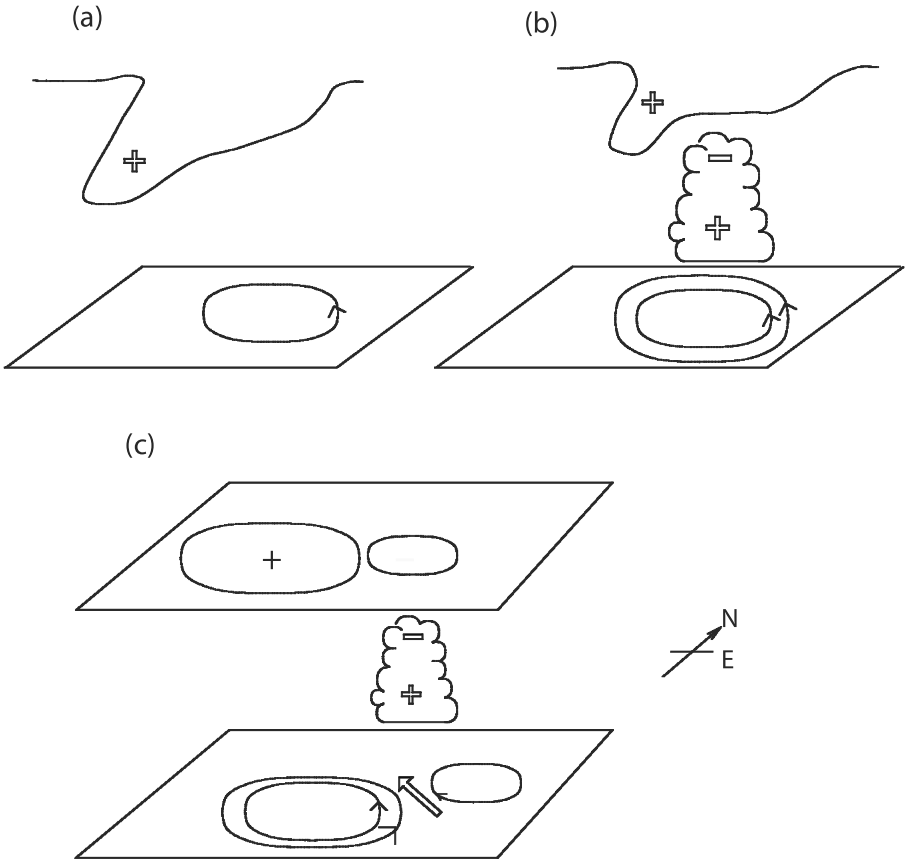

Figure 7. Schematic illustration of the various effects of latent heat release on the low-level circulation associated with upper level potential vorticity anomalies. (a) The situation with no latent heat release. The upper line denotes a tropopause fold, with associated positive PV anomaly. A low-level, cyclonic circulation is induced. (b) The dominant effects of latent heating. A positive low-level anomaly is formed which intensifies the low-level circulation. A local sink of PV is located above and erodes the upper level feature. (c) A subsidiary effect of latent heat release. A downstream ridge is generated and is associated with weak, downstream anticyclonic flow. (From *Ahmadi-Givi et al.* [2004], ©Royal Meteorological Society, reprinted with permission.)

that weaken the low-level fields attributable to the upper level feature." In order to really separate the different types, an approach that takes the latent heating into account is necessary. Both *Ahmadi-Givi et al.* [2004] and *Plant et al.* [2003] used a piecewise PV inversion technique to quantify the influence of different PV features. This involves calculating geopotential height fields from individual PV features in the field, for example, upper level or lower level features.

The influence of diabatic heating on the development of Type C cyclones was described for a case study in *Ahmadi-Givi et al.* [2004] and is shown schematically in Figure 7. In this case the cyclone was initiated by an upper level PV anomaly when there was almost no low-level temperature anomaly. During the development, a low-level PV anomaly developed due to latent heat release, and the induced cyclonic circulation generated a temperature anomaly. The temperature anomaly played very little role in the intensification of the cyclone, whereas the upper level PV anomaly and the latent heating-induced low-level PV anomaly contributed similarly toward the mature stage of the cyclone life cycle. The outflow at upper levels acted to weaken the upper level PV anomaly and contributed to downstream ridge development. This interaction can explain the increasing tilt with height found in Type C cyclones by *Deveson et al.* [2002]. In fact, the downstream impact of outflow from extratropical cyclones, particularly the WCB, which reaches upper levels with anticyclonic PV anomalies due to the latent heat release is now widely recognized [*Madonna et al.*, 2014a, 2014b; *Schemm and Wernli*, 2014].

Graf [2014] performed a principal component analysis on 30 cyclogenesis precursors for extratropical cyclones in the NH in order to classify them. Without prior selection of the most important features, the

statistical technique identified upper level and lower level PV anomalies as good distinguishers between cyclogenesis events in their classification scheme. The low-level PV anomalies were found to be associated with moist dynamics, and cyclogenesis events associated with these anomalies are not represented by the classification of *Petterssen and Smebye* [1971].

During FASTEX the performance of weather forecasts related to the studied cyclones was investigated by *Clough et al.* [1998] and summarized according to type by *Deveson et al.* [2002]. Type A cyclones were found to be well forecast, whereas type B and C cyclones were forecast quite well out to a lead time of 3 days; however, this depended on the scale of the cyclone, with larger ones easier to forecast [*Deveson et al.*, 2002]. The differences in forecast capabilities were attributed to various factors: the availability of observations to initialize the forecasts—this was much better for the type A cyclones since they are usually generated over the USA; the rate of development—type A cyclones typically evolve more slowly than type B or C; and spatial scale—with larger scales better forecast than smaller, which is potentially due to dissipation at upper levels in forecast models. Increased data assimilation into can increase the skill of those forecasts [*Deveson et al.*, 2002; *Irvine et al.*, 2011]. Continual improvements in satellite-observing systems and in situ observations will serve to increase forecasting capabilities.

3.4.2. Secondary Cyclones

While the studies of *Dacre and Gray* [2009] and *Gray and Dacre* [2006] only used frontal-wave cyclones from *Hewson* [1998], *Plant et al.* [2003] showed that nonfrontal lows can also be identified quite often as Type B or Type C (see Figure 8). However, the nonfrontal Type C cyclones tend to be more intense than the frontal-wave Type C cyclones. Conversely, frontal waves of Types A or B are more intense than their nonfrontal counterparts. Frontal wave cyclones in the eastern North Atlantic develop in an environment with weaker temperature gradients, lower static stability, and stronger upper level PV anomalies [*Dacre and Gray*, 2013; *Schemm and Sprenger*, 2015], further indicating the importance of diabatic heating.

Secondary frontal-wave cyclones tend to be of much smaller scale and can develop more rapidly than primary cyclones [*Parker*, 1998]. One well-documented example of such explosive development of a secondary frontal-wave cyclone is the Great Storm of October 1987 [*Hoskins and Berrisford*, 1988; *Shutts*, 1990], which hit the United Kingdom causing extensive damage. The smaller scale means that these cyclones are likely to be more readily influenced by diabatic processes [*Parker*, 1998]. *Rivals et al.* [1998] showed the importance of the link between diabatic PV anomalies and upper level anomalies (a tropopause fold) in the initiation of a secondary frontal-wave cyclogenesis event.

The three types of frontal-wave secondary cyclogenesis described by *Sawyer* [1950] were thought by *Thorncroft and Hoskins* [1990] to be variations on the relative location of the upper level PV anomaly to the surface fronts. In the study of *Thorncroft and Hoskins* [1990], the upper level PV anomaly that caused the secondary cyclogenesis originated due to the anticyclonic RWB seen in LC1 [*Thorncroft et al.*, 1993]. Considering the North Atlantic region, this anticyclonic RWB takes place mostly over the East Atlantic [*Gómara et al.*, 2014], a region known for its secondary cyclogenesis.

The objective identification of fronts and frontal-wave cyclones provides an opportunity to separate out these features as a different class of cyclones. Recent objective identification of frontal-wave cyclogenesis finds that only between 8 and 14% of cyclogenesis events (depending on the location within the North Atlantic region) meet this definition [*Schemm and Sprenger*, 2015], which is lower than the percentage seen in *Plant et al.* [2003]. *Hewson and Titley* [2010] developed a method to identify the full range of cyclones and their life cycles with three types specified: diminutive frontal waves, frontal waves, and barotropic lows. Many objective cyclone identification and tracking algorithms employ various thresholds, including a lifetime threshold [*Neu et al.*, 2013], which could result in a number of the most rapidly developing cyclones being missed.

3.4.3. Upper Level Flow Features

Motivated by the lack of studies on the SH and the recent increased availability of satellite-derived atmospheric data, *Sinclair and Revell* [2000] performed a manual classification of 40 developing cyclones in the Southwest Pacific region centered on New Zealand, that were identified using the cyclone identification and tracking method of *Sinclair* [1997]. This classification was based on upper level flow configurations at the time of cyclogenesis and yielded four distinct classes: (1) The so-called trough class (T), where the cyclogenesis occurs below a deep upper level trough quite far from the upper level jet streak; (2) the upstream exit class (U), where the cyclogenesis occurs in the poleward exit region of the upper level jet streak that is upstream of the

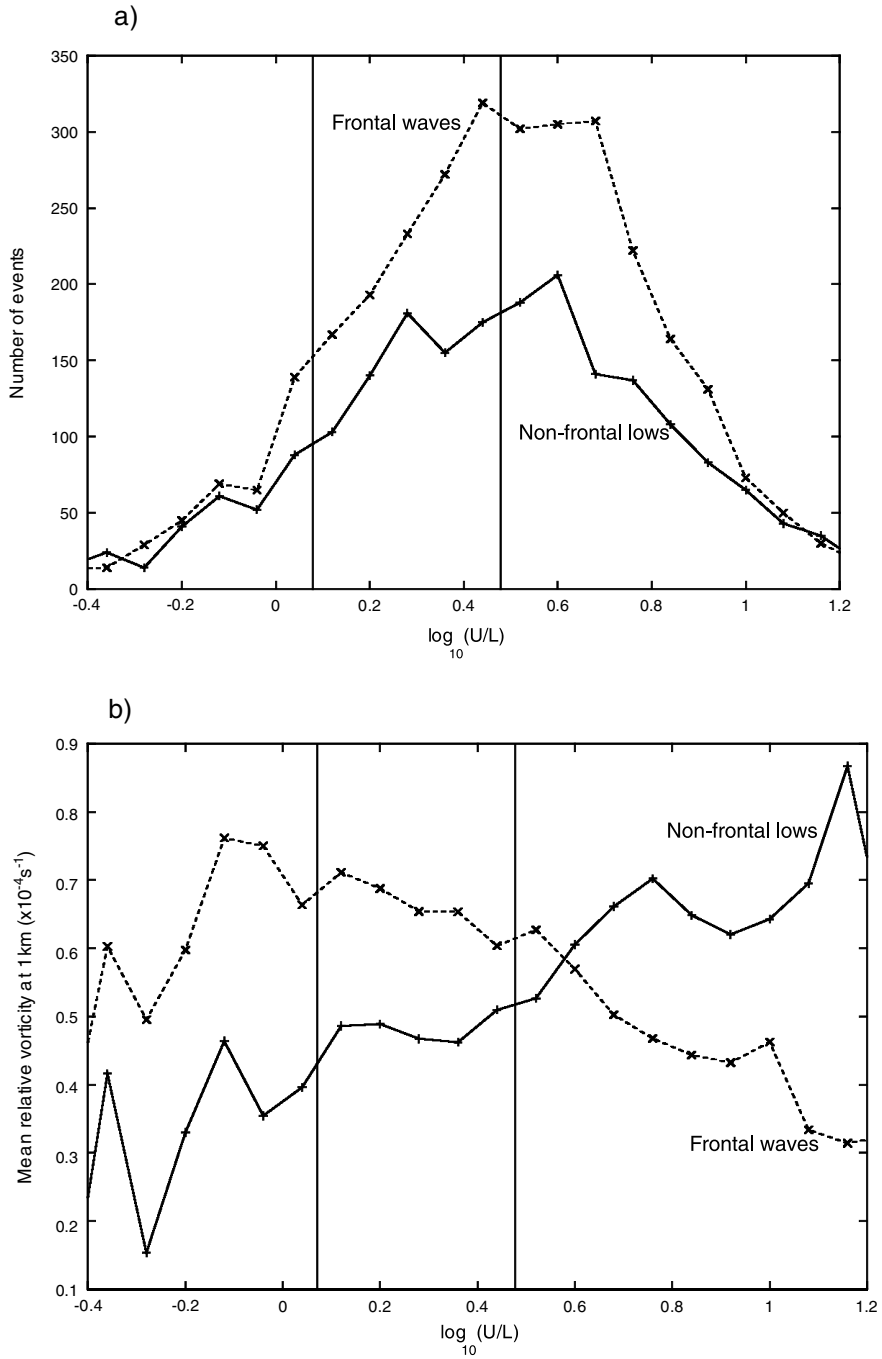

Figure 8. Results from the analysis of a database of cyclonic features, containing a total of 3199 frontal waves and 2099 nonfrontal lows. The features of each type are grouped into bins according to the instantaneous U/L ratio, with $\delta \log_{10}(U/L) = 0.08$ (equation (1)). (a) The number of events of each type, with symbols plotted at the center of each bin. (b) The mean of the 1 km relative vorticities for the events in each bin. In both cases,vertical lines are added, drawn along the $\log_{10}(U/L)$ thresholds of *Deveson et al.* [2002]. (From *Plant et al.* [2003], ©Royal Meteorological Society, reprinted with permission.)

upper level trough; (3) the downstream exit class (D), which is similar to the upstream exit but the upper level trough is downstream of the jet streak; and (4) the equatorward entrance class (E), where the cyclogenesis occurs on the equatorward side of the upper level jet streak that is downstream from the upper level trough.

In their study *Sinclair and Revell* [2000] attempted to identify the most similar satellite-based classes from *Evans et al.* [1994]. Class E was found to most resemble the instant occlusion from *Evans et al.* [1994], class U

resembles the comma cloud, class D resembles the left exit (although in the SH this is equivalent to the right exit), and class T does not resemble any of the classes from *Evans et al.* [1994].

3.4.4. Other Cyclone Features

A number of studies have produced climatologies of Mediterranean cyclones [e.g., *Trigo et al.*, 1999; *Maheras et al.*, 2001; *Flocas et al.*, 2010]. *Campins et al.* [2000] presented a classification of western Mediterranean cyclones using a *k*-means clustering technique based on inputs of cyclone intensity (as the Laplacian of pressure) and measures of the shape of the pressure pattern (symmetry and the eccentricity). Using this technique, *Campins et al.* [2000] describe seven classes of western Mediterranean cyclones with most having their genesis related to orographic features and some related to thermal lows or baroclinicity.

A dynamical technique of *Fita et al.* [2006] investigated the differing roles of the upper level, lower level, and diabatically produced PV anomalies in a number of intense Mediterranean cyclogenesis events. For the 11 cases that they considered, the upper level PV anomaly was generally the primary factor in the cyclogenesis. The low-level thermally generated PV anomaly was of secondary importance, and the diabatically generated PV anomalies even less important. However, as the authors state, the diabatically generated PV anomalies did not include the direct diabatic forcing. Although the *Fita et al.* [2006] study did not classify the cyclones and only considered a small number, this type of method could be used on a larger number of cyclones to classify them according to the relative importance of the different PV anomalies. The "dynamic" PV-based prognostic system of *Romero* [2008] offers the opportunity to further understand the role of different PV anomalies in cyclone development (including upper and lower levels, latent heating, and orographic) in order to produce a classification of a climatology of cyclones. *Romero* [2008] suggests that the Mediterranean would be a good region in which to apply this method, although it could also be extended to other regions.

3.5. Transitioning Extratropical Cyclones

Many of the classification studies described above involve the diagnosis of the dynamics of (or the cloud features associated with) cyclogenesis. There is a class of extratropical cyclones that have a different origin—those that transition from a tropical cyclone into an extratropical cyclone.

Extratropical transition (ET) occurs in the Northwest Pacific, the Northwest Atlantic, the Indian Ocean, and Southwest Pacific tropical cyclone regions [e.g., *Klein et al.*, 2000; *Hart and Evans*, 2001; *Sinclair*, 2002; *Jones et al.*, 2003], and the first identified tropical cyclone in the South Atlantic also transitioned [*Pezza and Simmonds*, 2005; *McTaggart-Cowan et al.*, 2006]. ET is the process by which a tropical cyclone loses its tropical characteristics and gains more features of an extratropical cyclone. This occurs when the tropical cyclone interacts with the midlatitude westerlies, and as such, its translation speed increases. The cyclones tend to change from warm-core symmetric systems with strong convection to cold-core asymmetric systems with frontal cloud and precipitation structures from the start of their transition to the end. *Klein et al.* [2000] developed a conceptual model of ET in the Northwest Pacific which explains the environmental factors that give rise to ET. As a tropical cyclone moves poleward, it experiences cooler sea surface temperatures (SST), stronger SST gradients, and increased baroclinicity and vertical shear, which all contribute to the development of the asymmetric structure of cloud and precipitation.

These types of events can have large socioeconomic impacts due to their heavy rain [e.g., *DiMego and Bosart*, 1982; *Atallah and Bosart*, 2003] and intense winds [e.g., *Evans and Hart*, 2008]. The transition of Hurricane Sandy in 2012, coupled with its immense size and its path, resulted in a disastrous storm surge of up to 3.8 m (measured in New York [*Blake et al.*, 2013]). Transitioning tropical cyclones can also have large downstream impacts on the midlatitude circulation through upper level PV modification [*Grams et al.*, 2013a, 2013b; *Archambault et al.*, 2013].

Although ET may be thought of as a particular class of cyclones when compared to other extratropical cyclones, there have also been a number of studies that have classified different types of ET. These studies are summarized in *Jones et al.* [2003] and typically are based on how the tropical cyclone interacts with the midlatitude flow. One of these classes involves tropical cyclones decaying and their PV remnants interacting with a midlatitude trough or baroclinic zone, producing cyclogenesis and growth consistent with Type B cyclogenesis (see section 3.4). The others involve interaction with surface fronts or surface low pressure systems in the midlatitudes.

Hart [2003] developed a phase space diagnostic that can be used to track the development of ET from warm-core symmetric systems to cold-core asymmetric systems using low-level thickness asymmetry and

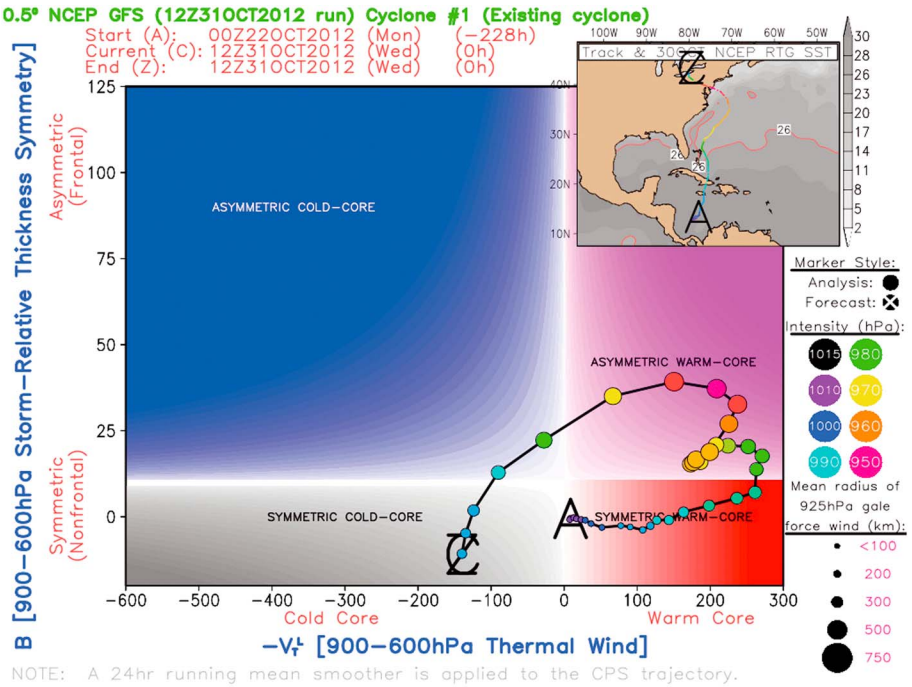

Figure 9. Cyclone phase space (CPS) diagram for Hurricane Sandy derived from the National Center for Environmental Prediction (NCEP) Global Forecasting System (GFS). The horizontal axis shows the thermal wind from 900hPa to 600hPa (negative indicates a cold-core system, and positive indicates a warm-core system). The vertical axis shows a measure of the asymmetry of the system (high values indicate an asymmetric or frontal system, low values show a symmetric system more akin to a tropical cyclone). Inset at top right shows the track and the sea surface temperature (SST; °C). Reprinted with permission from https://www2.ucar.edu/sites/default/files/news/2012/1.phase1%20copy.jpg.

thermal wind. An example of this is shown for Hurricane Sandy in Figure 9, which reintensified in the midlatitudes as a warm seclusion cyclone [*Galarneau et al.*, 2013]. (Extratropical cyclones developing warm seclusions maintain a cold core at higher levels [*Hart*, 2003].) Based on this idea, *Studholme et al.* [2015] developed an objective way of classifying the extratropical transition of systems with a view to being able to apply this to climate model output. They found that about half of all identified NH tropical cyclones at least began transition. Objective tropical cyclone identification methods can be useful for analyzing ET as they tend to track the systems further into the midlatitudes than track information from forecast centers in some regions [*Strachan et al.*, 2013].

3.6. Subtropical Cyclones and East Coast Lows

In general, the environmental conditions in the subtropics suppress the development of cyclones [*Yanase et al.*, 2014; *Yanase and Niino*, 2015]. Extratropical cyclones tend not to develop in the subtropics due to weak baroclinicity. The idealized simulations of *Davis* [2010] show that if there is sufficient vertical wind shear, and latent heating due to convection, subtropical cyclones can form even without strong surface baroclinicity. Observational studies show that there are certain types of cyclones that occur in these regions at different times of the year.

Otkin and Martin [2004] produced a climatology of subtropical storms in the central and eastern Pacific in the NH (also called Kona Storms). These are systems that occur predominantly in the cool season (from October to March) and propagate mostly to the northeast. Subtropical storms in this region are suppressed in midwinter, and most occur in the late autumn and late winter/early spring, which is similar to the climatology of all Pacific extratropical cyclones [*Penny et al.*, 2009; *Nakamura*, 1992]. *Otkin and Martin* [2004] subjectively split identified storms into three classes as follows:

1. The first involves the development of the cyclone along an equatorward extruding cold front and subsequent propagation in a predominantly eastward direction (named CFC).
2. The second type occurs when a cyclone develops along a cold front and moves mostly westward (named CT).
3. The third occurs when a cyclone develops in low-level easterlies with no associated cold front (named TWE).

The features of the genesis and development of these different classes are related to the location of these Kona cyclones relative to the midlatitude westerlies and the subtropical ridge. CFC cyclones develop under an upper level trough within the westerlies, associated with strong baroclinicity. CT cyclones develop on the equatorward edge of the subtropical ridge, still within high baroclinicity. Finally, TWE cyclones develop in a region with weak temperature gradients and trade wind easterlies.

The climatology of subtropical storms in the North Atlantic developed by *Evans and Guishard* [2009] and *Guishard et al.* [2009] considered only the hurricane season, and so these storms are somewhat different to those of *Otkin and Martin* [2004] who consider the full year. *Evans and Guishard* [2009] specify a number of criteria that a storm should meet in order to be considered a subtropical storm: (1) The presence of gale force winds; (2) A hybrid structure (warm core at low levels and cold core at upper levels, defined using the *Hart* [2003] cyclone phase space criteria) for at least 36 h; (3) The development between 20° and 40°N and tracked only over the ocean; and (4) The requirement to not be identified as a tropical cyclone or extratropical cyclone for more than 24 h prior to attaining its hybrid structure (for example, in the case of extratropical transition or a warm seclusion extratropical cyclone).

One requirement for the development of subtropical storms is the presence of an upper level PV anomaly [*Otkin and Martin*, 2004; *Guishard et al.*, 2009]. In the Atlantic, if the subtropical storm develops over warm enough water, it may develop sufficient convection to become a deep warm-core structure and further develop into a tropical cyclone.

One particular type of subtropical cyclone occurs to the east of Australia and is known as an East Coast Low (ECL). ECLs tend to be cool season phenomena (occurring April–September) and are considered to be extratropical cyclones [*Dowdy et al.*, 2013a]. These cyclones can be particularly damaging due to their rapid development, strong winds, high seas, and heavy precipitation [e.g., *Abbs et al.*, 2006; *Mills et al.*, 2010]. The development of ECLs is associated with an upper level PV anomaly, in much the same way as the subtropical features mentioned above. Another similarity with subtropical cyclones mentioned above is the observed shallow warm core [*Mills*, 2001].

The potential for ECL development can be identified using large-scale upper level diagnostics [*Dowdy et al.*, 2013a], impacts such as precipitation [*Hopkins and Holland*, 1997], manually using weather charts [*Speer et al.*, 2009] or automated cyclone identification, and tracking methods including some mean sea level pressure (MSLP) deepening criteria [*Pepler and Coutts-Smith*, 2013; *Browning and Goodwin*, 2013; *Pepler et al.*, 2015]. All methods tend to identify the observed ECLs with the largest impacts [*Pepler et al.*, 2015].

Even within this small region, there can be different classes of ECLs and *Holland et al.* [1987] described their classification based on the location of the cyclogenesis relative to an easterly dip (where a trough develops equatorward of an anticyclone; see schematic diagram in Figure 10). Type 1 occurs when an easterly dip forms over the Australian continent and tends to be very small (only around 100 km across). Type 2 ECLs tend to be larger features that develop on the easterly dip axis, which can develop rapidly and produce heavy precipitation and strong winds. Type 3 are also very small, short-lived features that occur when the easterly dip is further east of the Australian coast.

Both ECLs and Kona storms develop in regions of low-level easterlies, equatorward of the subtropical ridge. For Kona storms, most cases require the low-level baroclinicity associated with a decaying cold front, whereas in ECLs it may be that the baroclinicity is provided by the strong SST gradients at the Australian East Coast. CT and TWE cyclones are similar to the easterly dip of ECLs and strongly resemble the schematic shown in *Holland et al.* [1987] and Figure 10.

The relatively small scale of ECLs (sometimes as small as 50 km across) means that high resolution is required to simulate them [*Leslie et al.*, 1987]. High-resolution SST data used as boundary conditions for model simulations give better representation of the precipitation structure [*Chambers et al.*, 2014]. Regional models are able to capture ECL occurrence [*Pepler et al.*, 2016], while for lower resolution GCMs, the large-scale diagnostics of *Dowdy et al.* [2013a] may be a good indicator of ECL activity [*Dowdy et al.*, 2013b].

3.7. Polar Lows

While extratropical cyclones can propagate into, or may develop in, the high-latitude regions [e.g., *Zhang et al.*, 2004; *Serezze*, 1995; *Simmonds et al.*, 2003], another distinct type of system, referred to as a polar low, can occur at high latitudes (i.e., poleward of 60°). Polar lows are intense, mesoscale cyclones that typically form during cold-air outbreaks—when very cold air passes over relatively warmer seas [*Rasmussen and Turner*, 2003].

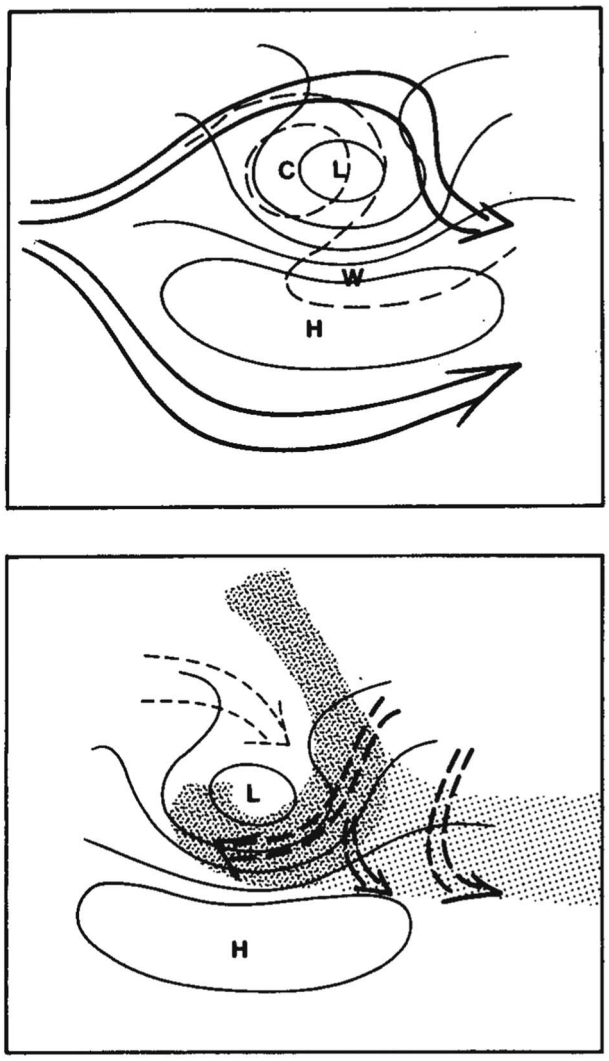

Figure 10. Schematic of the major features of an easterly dip: (top) Surface isobars (solid lines), 100–500hPa thickness contours (dashed lines), and the diffluent upper tropospheric jet streaks (long arrows); (bottom) Surface isobars, stratiform cloud with embedded convection (heavy stipple), stratiform cloud (light stipple), and wet bulb potential isentropic trajectories with downward motion along the dashed arrow and upward motion along the broken arrows. (From *Holland et al.* [1987], ©American Meteorological Society, reprinted with permission.)

Baroclinicity, latent heating, the interaction of surface fluxes with latent heating, and upper level disturbances (e.g., PV anomalies) have all been shown to be important mechanisms in the development of polar lows [*Rasmussen*, 1979; *Nordeng*, 1987; *Emanuel and Rotunno*, 1989; *Grønås and Kvamstø*, 1995; *Yanase and Niino*, 2005, 2007; *Terpstra et al.*, 2015]. Satellite imagery reveals that polar lows can resemble tropical cyclones, with a cloud-free eye and spiraling cloud bands [e.g., *Rasmussen*, 1981] or extratropical cyclones, with a comma cloud structure [e.g., *Reed. and Duncan*, 1987]. The structure of the cloud features associated with polar lows seems to depend partly on the strength of the baroclinicity; in a strongly baroclinic environment the polar lows tend to be bigger and with a comma cloud; when baroclinicity is weak the polar lows tend to develop a more tropical cyclone-like appearance (from idealized modeling [*Yanase and Niino*, 2005, 2007]). Nevertheless, observations show that tropical cyclone-type features can occur in polar lows initially developing in a baroclinic environment [*Forbes and Lottes*, 1985].

Recently, *Terpstra et al.* [2016] classified polar lows in the Norwegian Sea according to whether they developed in forward shear (where the mean and thermal wind are in the same direction) or reverse shear (where the mean and thermal wind are in opposite directions). The forward shear case resembles a typical baroclinic

structure with the strongest winds at upper levels. The reverse shear is quite distinct, with a strong low-level jet and resultant stronger surface fluxes.

Satellite imagery has been used to identify and produce climatologies of polar lows [*Businger*, 1985; *Carleton and Carpenter*, 1990; *Blechschmidt*, 2008; *Noer et al.*, 2011] and also to classify them [*Forbes and Lottes*, 1985]. Recently, a number of objective methods have been used to identify and track polar lows from gridded data (observational analyses, reanalyses, or downscaled reanalysis) in the North Atlantic [*Zahn and von Storch*, 2008], the Norwegian Sea [*Zappa et al.*, 2014], and in the Japan Sea [*Yanase et al.*, 2016]. Due to strict criteria in vertical temperature structures, or propagation directions, these methods may not identify all cases of forward shear polar low genesis [*Terpstra et al.*, 2016]. The underestimation of objectively identified polar lows (compared to a satellite-based data set [*Zappa et al.*, 2014]) in the European Centre for Medium Range Weather Forecasting (ECMWF) reanalysis data set (ERA-Interim) [*Dee et al.*, 2011], which has a resolution of approximately 0.75°, suggests that these types of features may not be represented in climate models.

3.8. Classification Based on Impacts

3.8.1. Winds

One of the major impacts of extratropical cyclones that has received a lot of attention (in Europe especially) is the wind damage. Synoptic-scale variability in surface winds is strongly related to the midlatitude storm tracks and the regions of maximum atmospheric instability [*Booth et al.*, 2010]. The winds associated with extratropical cyclones can be extreme [e.g., *Nissen et al.*, 2010; *Raveh-Rubin and Wernli*, 2015] and can cause widespread damage over Europe (and elsewhere) and thus are a very costly natural hazard [e.g., *Fink et al.*, 2009]. Losses can be estimated using information on the daily maximum gust wind speeds [*Klawa and Ulbrich*, 2003]. The gusts themselves can be hard to measure and predict; therefore, methods have been developed to estimate them from larger-scale wind information using dynamical and statistical approaches [*Born et al.*, 2012; *Haas and Pinto*, 2012]. *Roberts et al.* [2014] produced a catalog of extratropical cyclones with strong winds over Europe containing information on 3 s gusts obtained from high-resolution modeling. The winds associated with extratropical cyclones (especially on the U.S. East Coast) can also cause extensive damage from large storm surges [*Colle et al.*, 2015, and references therein].

Hewson and Neu [2015] developed a new conceptual model of the strongest winds in extratropical cyclones, finding three particular regions with distinct features (Figure 11): the warm conveyor belt jet (WJ), the sting jet (SJ), and the cold conveyor belt jet (CJ). Not all features are necessarily present in every extratropical cyclone, but typically, the WJ develops early in the life cycle along the cold front, within the warm sector of the cyclone. The sting jet, first described by *Browning* [2004], occurs at the end of the bent-back front as high momentum air descends from the cloud head into a region of frontal fracture. The SJ is the smallest and shortest-lived of the wind features, but the most damaging. The CJ occurs on the cold side of the warm front, typically forming just before the minimum cyclone pressure. The location of the maximum winds either in the warm sector or on the cold side of the warm front during different stages of the cyclone life cycle can be related to the interaction of the cyclone-related winds with the large-scale winds and the redistribution of eddy kinetic energy [*Rivière et al.*, 2015].

Hewson and Neu [2015] also address the question of whether relatively low-resolution data sets (such as ERA-Interim) can represent the WJ, CJ, and SJ features. The wind gusts associated with the WJ and CJ are usually well represented in ERA-Interim, but the SJ is not represented (due to its spatial scale). *Martinez-Alvarado et al.* [2012] showed that many intense cyclones, identified in reanalysis data, with high values of slantwise convective instability in the North Atlantic region, develop a sting jet when simulated with a high-resolution model (the Met Office Unified Model).

A number of identification methods for severe winds associated with extratropical cyclones have been developed [e.g., *Leckebusch et al.*, 2008; *Nissen et al.*, 2010; *Booth et al.*, 2015]. *Nissen et al.* [2010] identified and tracked extreme wind events, defined as regions with winds exceeding the local 98th percentile, and linked these regions to nearby cyclones. They only considered features larger than three grid boxes (with resolution of 1.125°) and with lifetimes greater than 18 h; therefore, it is likely that this method would only pick up the WJ and the CJ from the conceptual model of *Hewson and Neu* [2015]. This type of feature tracking would be a very useful tool in the identification of these wind features in reanalysis and model data and could be combined with diagnostics of the air masses to compare climatologies of WJ and CJ features.

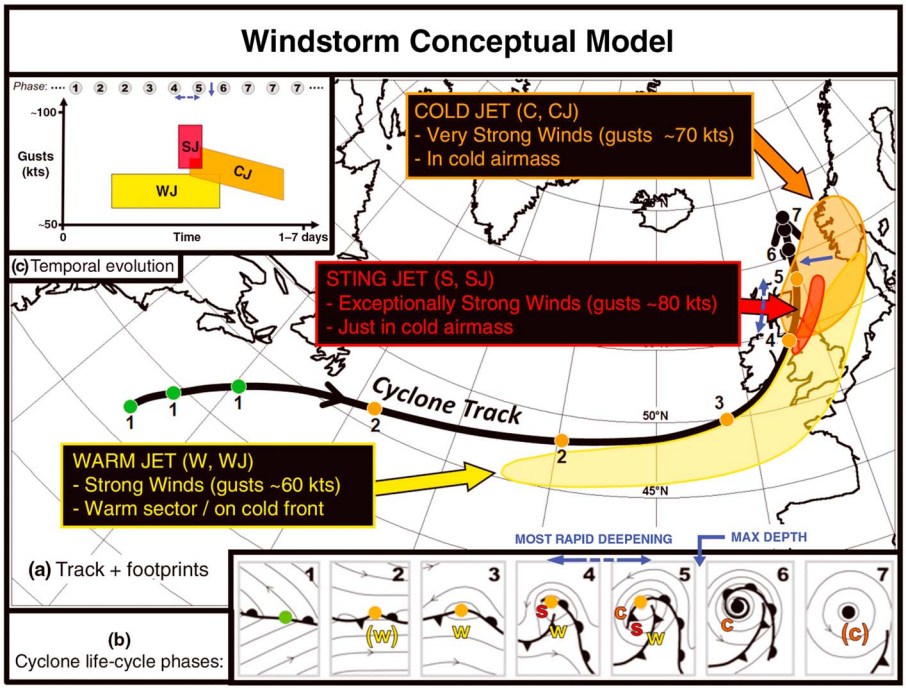

Figure 11. Conceptual model of an extratropical cyclonic windstorm. (a) The cyclone track (black), with spots denoting positions equally separated in time, and numbered according to the cyclone life cycle phases in Figure 11b. Spot color relates to the identification method and objective typing used in *Hewson and Titley* [2010], green being a diminutive frontal wave, orange a frontal-wave cyclone, and black a barotropic low. Shading denotes the footprints, or nominal damage swathes, attributable to the warm jet/warm conveyor (yellow), the cold jet/cold conveyor (orange), and the sting jet (red). (b) The synoptic-scale evolution of fronts and isobars around the cyclone, after *Hewson and Titley* [2010] and *Shapiro and Keyser* [1990], with added letters denoting relative locations of the strong wind features and brackets indicating marginal existence. (c) The temporal evolution of gust strength for each jet zone, with numbers cross-referencing phases on Figure 11b. On each panel, a dashed blue line denotes the period of most rapid deepening, while the solid blue arrow shows the time of maximum depth. From *Hewson and Neu* [2015], licensed under CC BY 4.0 (http://creativecommons.org/licenses/by/4.0/legalcode).

3.8.2. Precipitation

The other major impact associated with extratropical cyclones comes from the (often very heavy) precipitation. Extratropical cyclones and their associated fronts have been shown to be associated with a very large proportion of precipitation in the midlatitudes (up to 90% in some regions [*Hawcroft et al.*, 2012; *Catto et al.*, 2012]), as well as the most extreme precipitation events [*Pfahl and Wernli*, 2012; *Catto and Pfahl*, 2013; *Kunkel et al.*, 2012]. Many flooding events have been associated with atmospheric rivers in Europe [*Lavers et al.*, 2011] and the USA [*Ralph et al.*, 2006], which are also important features of the midlatitude climate. *Sodemann and Stohl* [2013] found that a number of cyclones can feed off the moisture in atmospheric rivers, whereas *Dacre et al.* [2015] found that the "sweeping up" of moisture by cyclones produces atmospheric rivers. The direction of the linkage between individual cyclones and long-lasting atmospheric rivers is therefore uncertain, but there could be some benefit in investigating the different impacts of cyclones associated or not associated with atmospheric rivers.

The spatial distribution and magnitude of precipitation in extratropical cyclones vary according to cyclone strength and moisture availability [*Field and Wood*, 2007; *Pfahl and Sprenger*, 2016] and by ocean basin and season [*Chang and Song*, 2006]. The studies of *Chang and Song* [2006] and *Field and Wood* [2007] used only temporal snapshots of cyclones (rather than considering their full life cycle) and made use of cyclone-centered compositing in their analysis. *Pfahl and Sprenger* [2016] considered different times in the cyclone life cycle and found that the precipitation occurring before the time of maximum intensity was more strongly related to the cyclone strength than the precipitation occurring afterward, indicating the importance of the contribution of the latent heating from precipitation in the cyclone intensification. The inclusion of this type of life cycle information and consideration of the precipitation distribution in cyclones of different types (e.g., the threefold

classification scheme of *Deveson et al.* [2002]) could add further to the understanding of precipitation in extratropical cyclones.

3.8.3. Clustering

The socioeconomic impacts of extratropical cyclones are greatly enhanced by what is termed the "serial clustering" of cyclones [e.g., *Mailier et al.*, 2006], which can occur over western Europe [*Ulbrich et al.*, 2001; *Fink et al.*, 2009]. These clustering events are strongly controlled by the large-scale flow and particularly Rossby wave breaking [*Pinto et al.*, 2014]. Often, such clustering is associated with secondary cyclogenesis (see section 3.4.2) along the trailing cold front of a parent cyclone (therefore resembling the cyclone families suggested by *Bjerknes and Solberg* [1922]). While the cyclones occurring in a cluster may exhibit different features, understanding of the processes behind what makes them occur is important in considering future changes.

4. Climate Modeling

There has been a recent increase in the number of climate model evaluation studies using "process-based" techniques (i.e., evaluating individual processes or weather features within the models). This comes from recognizing that even if a climate model has an excellent mean state, the weather systems making up this climate may be incorrectly simulated. Ultimately, the future climate changes we experience will depend on changes on the scale of individual weather events.

First in this section, an overview of the representation of the midlatitude storm tracks (i.e., the preferred regions of cyclones) is given. Then model evaluation studies that make use of the classification ideas presented in section 3 are identified. Model evaluation studies where classification methods could (and should) be used to give greater insight into climate model processes are also highlighted. Finally, studies evaluating the representation of climate processes that need to be represented in order to simulate different classes of cyclones correctly are detailed.

4.1. Representation of the Storm Tracks

Extratropical storm tracks have been evaluated in climate models using two main methods. The first is using Eulerian measures such as mean sea level pressure variability or eddy kinetic energy [e.g., *Blackmon et al.*, 1977]; and the other is the objective identification and tracking of individual cyclones [e.g., *Neu et al.*, 2013], which allows a comparison of track statistics and spatial distribution. These methods have been used to show that climate models capture the characteristics of storm tracks [e.g., *Ulbrich et al.*, 2008; *Catto et al.*, 2011; *Colle et al.*, 2013; *Zappa et al.*, 2013] and show improvements over earlier models [*Löptien et al.*, 2008]. The exact systems identified by different objective tracking methods can differ [*Neu et al.*, 2013], and care needs to be taken when comparing results from different studies. The most recent Intergovernmental Panel on Climate Change (IPCC) report (AR5) summarized the evaluation of extratropical storm tracks and cyclones [*Flato et al.*, 2013] and found that overall the representation of these features in climate models is improving over time.

4.2. Making Use of Classifications

Some of the ideas and techniques from the cyclone classifications detailed in section 3 have been used to aid in some model evaluation studies. Such studies are now considered.

4.2.1. Cyclone Structure

Catto et al. [2010] used feature tracking and cyclone-centered compositing to find that a high-resolution climate model could capture the three-dimensional dynamical features of extratropical cyclones at their time of maximum intensity. This study used the conceptual airflow ideas (discussed in section 3.3) to inform the comparison between reanalysis and model data. The model exhibited problems with the distribution of cloudy areas; however, this same model has since been found to represent average cyclone-related precipitation fairly well [*Hawcroft et al.*, 2015]. (This model, the High Resolution Global Environment Model (HiGEM) [*Shaffrey et al.*, 2009], has a resolution of 0.83° latitude × 1.25° longitude. The resolution of models included in the Fourth Assessment report of the IPCC in 2007 (AR4) ranged from 1.1° to 5°.)

4.2.2. Explosive Cyclones

The spatial distribution of explosive cyclones is well represented by the CMIP5 models, but the frequency is underestimated [*Seiler and Zwiers*, 2015]. This is strongly related to biases in jet stream speed and may also be associated with jet stream orientation, SST biases (particularly gradients of SST in the Gulf Stream and Kuroshio Current regions), and Eady growth rate. Model resolution is an important factor in the frequency of

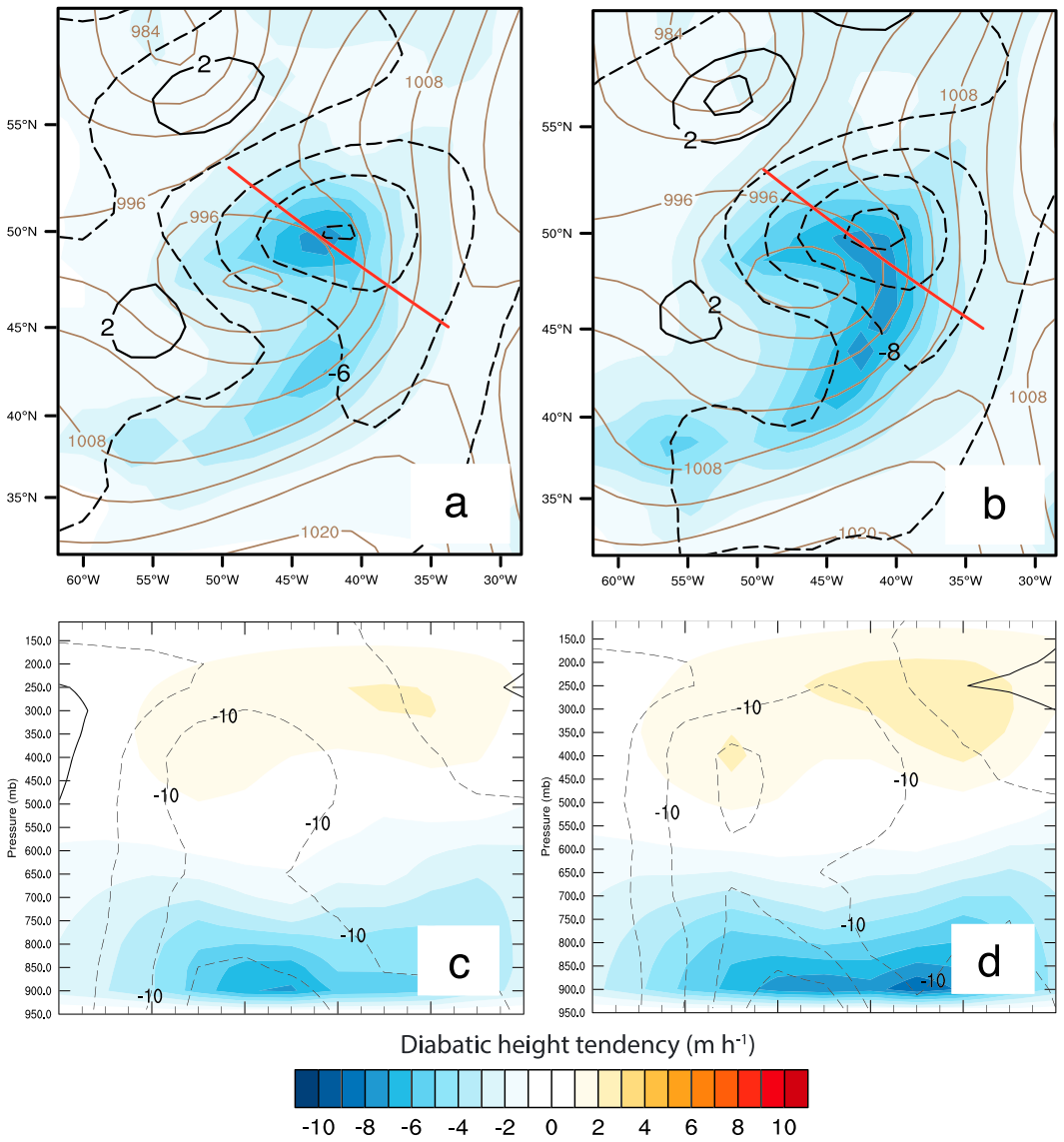

Figure 12. Diabatic height tendency (shaded, m h^{-1}), total geopotential height tendency (dashed black contours, interval 5 m h^{-1}) at 850 hPa, and MSLP (brown contours, interval 4 hPa) for (a) 120 km and (b) 20 km grid spacing, 16 h into simulation with the Weather Research and Forecasting model (WRF) of a case study over the western North Atlantic at 0400 UTC 31 December 2001. Cross sections through red lines for (c) 120 and (d) 20 km grid spacing, with contours and colors as in Figures 12a and 12b. (From *Willison et al.* [2013], ©American Meteorological Society, reprinted with permission.)

explosive cyclogenesis, but this is only really clear when considering different resolution simulations with the same model [*Seiler and Zwiers*, 2015].

4.2.3. Precipitation Characteristics

Spatial patterns and annual average values of midlatitude precipitation are represented better than tropical precipitation in the CMIP5 models [*Flato et al.*, 2013]. Nonetheless, there has been a recent push to evaluate whether models are producing this precipitation for the right reasons (i.e., mainly associated with extratropical cyclones) and if the characteristics (such as the frequency and intensity) are as observed [*Sun et al.*, 2006]. For example, *Catto et al.* [2015b] evaluated precipitation associated with fronts in a number of CMIP5 models using an objective front identification method. While the overall frontal precipitation amount and the proportion of the total precipitation associated with fronts are quite well represented, this is due to complicated compensating factors, such as frontal precipitation that is too frequent (i.e., not enough dry fronts in

the models) and with an intensity that is too low. At higher intensities of frontal rainfall, the model precipitation matches better with the satellite estimates.

Hawcroft et al. [2015] find that one particular climate model has approximately the correct proportion of total precipitation associated with extratropical cyclones; however, the proportion linked to the strongest cyclones is too high in the model. Understanding of how these different precipitation characteristics contribute to (or indeed are caused by) dynamical differences in cyclone development would benefit from the consideration of different classes of cyclones as described in this paper (section 3). For example, in the threefold classification scheme [*Deveson et al.*, 2002; *Plant et al.*, 2003], it is likely that the type C cyclones requiring a large component of diabatic heating for their development, would be affected more by issues in the representation of precipitation and diabatic processes in models than type A or B.

The importance of diabatic processes for cyclone genesis and development increases in models with higher resolution [*Willison et al.*, 2013]. A comparison of the geopotential height tendencies (i.e., the intensification) of two cyclones simulated by a model with different resolutions shows the impact of this (Figure 12). The diabatic processes contribute a large proportion to the total height tendency, directly influencing the deepening of the cyclone. This is more pronounced in the simulation with higher horizontal resolution (20 km rather than 120 km), resulting in a cyclone that is more intense.

4.2.4. Wind Characteristics

Winds associated with cyclones have been evaluated by *Leckebusch et al.* [2006]. A multimodel statistical assessment of extreme winds in the CMIP5 models [*Kumar et al.*, 2014] shows that spatial patterns of extreme winds are well represented compared to ERA-Interim. Nevertheless, this does not take into account the cause of the extreme wind or how it relates to extratropical cyclones, and *Hewson and Neu* [2015] showed that even ERA-Interim does not represent all of the wind features associated with extratropical cyclones. To represent wind gusts at the surface, boundary layer processes must be represented well in models [*Hewson and Neu*, 2015].

4.2.5. Cloud Characteristics

Clouds in midlatitude weather systems can give information on the internal structure and dynamics of the systems (as shown in section 3.2) since different parts of the cyclone exhibit different cloud signatures. Satellite information, along with extratropical cyclone or identification and compositing methods, is being used to evaluate the cloud structures within climate models [e.g., *Field et al.*, 2008; *Naud et al.*, 2010; *Booth et al.*, 2013a; *Govekar et al.*, 2014]. This field is being somewhat driven by the large-scale temperature errors identified in climate models, supposedly caused by anomalous cloud radiative effects [*Trenberth and Fasullo*, 2010; *Bodas-Salcedo et al.*, 2012].

Govekar et al. [2014] find that one particular climate model underestimates the boundary layer clouds throughout their cyclone composites compared to satellite observations. Model cyclones that are too weak—particularly in the vertical velocity—lead to errors in the vertical distribution of clouds [*Naud et al.*, 2010; *Govekar et al.*, 2014]. *Govekar et al.* [2014] also found that the relationship between dynamical variables, such as the vertical velocity and the cloud properties are not well represented. Therefore, even if the model cyclones had the correct intensity, the clouds may still not be well represented. *Booth et al.* [2013a] find that another model also lacks low-level clouds, particularly related to fronts.

4.2.6. Extratropical Transition

ET is sensitive to a large number of processes and environmental conditions, making them very hard to forecast or simulate numerically [*Jones et al.*, 2003]. Among them are surface fluxes, orography, upper level trough structure, diabatic heating profile from convection, and large-scale precipitation. These are all aspects of climate model simulations that must be correct in order to be able to simulate ET correctly. Climate model resolution is extremely important for the representation of tropical cyclone intensity [*Strachan et al.*, 2013] and also improves the effect of orography of the flow [*Jung et al.*, 2006]. The parameterization of cumulus in models has been shown to be important for the simulation of ET [*Prater and Evans*, 2002], and the representation of clouds still presents many issues in climate models [*Bony et al.*, 2015].

4.3. Important Climate Features for Extratropical Cyclones

There are a number of climate features and physical processes that need to be represented well in climate models in order to produce the most realistic extratropical cyclones. A number of these features and how they are represented in models are given here.

This review has thus far shown that the underlying conditions (for example, the SSTs) are very important in development of cyclones [e.g., *Ludwig et al.*, 2014]. The strong SST gradients in the Gulf Stream and Kuroshio Current regions contribute to the baroclinicity of the atmosphere, and *Woollings et al.* [2010] find that the storm tracks are sensitive to the spatial and temporal resolution of the SST field. Biases in the storm tracks are reduced when higher-resolution SST fields are used *Woollings et al.* [2010]. The absolute values of the SSTs, as well as the gradient, can be important in controlling the intensity of cyclones over the Gulf Stream [*Booth et al.*, 2012] by providing moisture for latent heating. Many climate models, which typically have an atmosphere model coupled to an ocean model, exhibit SST biases that could impact on the storm tracks by producing biases in local SST gradients and hence baroclinicity [e.g., *Keeley et al.*, 2012]. Considering the influence in the other direction, cyclone-related winds are important for generating surface fluxes [*Zolina and Gulev*, 2003], and so this interaction must also be well represented in models.

Incorrectly simulating the SSTs may impact on some classes of cyclones more than others. For example, Types A and B cyclones from the threefold classification scheme [*Deveson et al.*, 2002] require a low-level baroclinic zone for their development and may therefore not be well represented in models with a weak SST gradient. Explosive cyclones are also sensitive to the underlying SST field [*Seiler and Zwiers*, 2015].

Since extratropical storm tracks are sensitive to the underlying SSTs, the ocean processes that influence these (e.g., the Atlantic Meridional Overturning Circulation; AMOC) must be well represented in coupled climate models [*Woollings et al.*, 2012]. Biases in the AMOC in models can alter the local SSTs in the North Atlantic region, thereby changing the baroclinicity and/or latent heating. *Chen et al.* [2013] find that the newest generation of climate models have improved their representation of the AMOC.

Low-frequency variability plays a large role in determining the location of the storm tracks. The regime analysis over the North Atlantic region by *Vautard* [1990] found that the synoptic-scale storm track extends much further over northwestern Europe during the "zonal" regime and into southwestern Europe during the "Greenland anticyclone" regime. This is also clearly seen in studies considering the impact of the North Atlantic Oscillation (NAO) on the storm tracks [*Hodges*, 2008]. During positive NAO events the North Atlantic storm track shifts to the north and has a more southwest to northeast tilt. Conversely, for the negative NAO index, the tracks are much more zonal with more cyclones propagating into the Mediterranean. When the storm tracks are shifted northward, they are more likely to be associated with WCBs [*Eckhardt et al.*, 2004] and to be stronger due to longer and more intense development phases [*Pinto et al.*, 2009]. The importance of WCBs for heavy rainfall [*Pfahl et al.*, 2014; *Catto et al.*, 2015a] suggests that northward shifted storms may have heavier associated rainfall.

Stoner et al. [2009] analyzed the models used in the IPCC fourth assessment report [*Randall et al.*, 2007] for their ability to simulate the spatial and temporal variability of a number of low-frequency modes. The NAO and two other high-latitude modes (the Pacific North American pattern (PNA) and the Arctic Oscillation (AO)) had spatial patterns that were represented well, although the temporal variability was not as good. *Lee and Black* [2013] looked at the simulated relationship between the NAO and the PNA patterns with the midlatitude storm tracks in the CMIP5 models. They found that, in general, the observed relationship was recreated, but differences between the models could be largely associated with differences in the mean state (i.e., the mean jet position). It would be useful to evaluate whether the models can capture the observed relationship between these low-frequency modes and certain cyclone characteristics.

Further afield, the El Niño – Southern Oscillation (ENSO) is a mode of tropical variability that has global impacts [e.g., *Dai and Wigley*, 2000]. SST anomalies in the tropical Pacific change the circulation of the tropics and force changes in the midlatitude jet stream and storm tracks [e.g., *Bengtsson et al.*, 2006; *Eichler and Higgins*, 2006]. *Bengtsson et al.* [2006] composited the NH tracking statistics from the winters with positive ENSO index (El Niño events) and those with negative index (La Niña events). The difference for El Niño minus La Niña from reanalysis data indicates a large response to ENSO over the East Pacific, with much higher track density in this region during El Niño. There is also a southward shift over the southern USA and into the North Atlantic, increasing the number of cyclones passing over the UK and northern Europe.

The representation of ENSO in climate models is improving [*Flato et al.*, 2013] and models can represent some aspects of teleconnections (such as the temporal variability) quite well [e.g., *Stoner et al.*, 2009]. However, there are still many issues with other simulated remote impacts, such as winds [e.g., *Schoof and Pryor*, 2014] and spatial variability of precipitation [*Langenbrunner and Neelin*, 2013].

In the SH the Southern Annular Mode (SAM) plays a large role in the variability of the storm tracks. A positive SAM index indicates a poleward contraction of the mean westerlies and negative SAM indicates an equatorward expansion. When the westerlies contract poleward, so do the main storm tracks. In this situation Australia receives fewer cyclones and passing fronts from the main storm track [*Rudeva and Simmonds*, 2015]. Similar effects are also seen in other regions of the SH [*Gillett et al.*, 2006]. Over Australia, however, there is an increased likelihood of cutoff lows forming during positive SAM, since atmospheric blocking is more likely to occur. The summary by the IPCC AR5 found that although climate models do show some variability similar to the SAM, there are issues with the exact spatial patterns [*Flato et al.*, 2013].

5. Future Projections

Future changes in the preferred locations of the extratropical storm tracks in a warming climate have received much attention in the literature due to their importance in the climate system and their socioeconomic impacts. This section will consider future projections of climate from three main perspectives. (1) The overall projections for the extratropical storm tracks and associated cyclones, (2) projections of certain classes of cyclones, and (2) projections of climate features of importance to extratropical cyclones and how these may affect the different cyclone classes.

5.1. Projections of the Storm Tracks

There have been a number of recent reviews of projected future changes in extratropical storm tracks and cyclones [*Ulbrich et al.*, 2009; *Kirtman et al.*, 2013; *Collins et al.*, 2013; *Colle et al.*, 2015; *Feser et al.*, 2015]. For the North Atlantic and Western Europe regions, the comprehensive review by *Feser et al.* [2015] finds no consistent trends in cyclone numbers; however, over the western North Atlantic a decrease in cyclone numbers is projected (see the review by *Colle et al.* [2015], and references therein). In the SH there is a robust signal of a poleward shift in the storm tracks in a warming climate [*Kirtman et al.*, 2013; *Collins et al.*, 2013], along with a consistent poleward shift and increase in upper level transient eddy kinetic energy [*Yin*, 2005]. The poleward forcing by increased greenhouse gases will be somewhat compensated by the equatorward forcing due to stratospheric ozone recovery [*Son et al.*, 2008; *Polvani et al.*, 2011; *Perlwitz*, 2011; *Purich and Son*, 2012]. Despite the robustness of certain results, there are still questions to be answered on the role of competing dynamical mechanisms in causing these projected changes (changes in available potential energy, for example [*O'Gorman and Schneider*, 2008]).

Feser et al. [2015] found that many studies consistently project increases in cyclone intensity over their regions of interest (e.g., the North Atlantic). Nevertheless, changes to cyclone intensities depend on the intensity measure. *Bengtsson et al.* [2009] and *Champion et al.* [2011] find increases in precipitation intensity in simulations from a single climate model using the A1B scenario from the IPCC AR4 (See Figure 13, which shows histograms of precipitation within cyclones); however, both studies also find no increased vorticity or winds associated with the increased precipitation, suggesting a lack of feedback between diabatic heating and cyclone intensity. These studies consider either all identified cyclones [*Bengtsson et al.*, 2009] or the extreme tails of the statistical distribution [*Champion et al.*, 2011] to compare their cyclones. This does not take into account that the cyclones being compared may belong to different classes (e.g., as shown in section 3) in the different time periods. This type of study would benefit from consideration of the different cyclone classifications detailed in this review. Idealized studies suggest that warmer or moister conditions act to increase the intensity of cyclones [*Booth et al.*, 2013b; *Pfahl et al.*, 2015], especially at the more intense end of the distribution [*Pfahl et al.*, 2015]. Such idealized studies do not take into account the rich spectrum of extratropical cyclone types and how they may respond differently to climatic change.

5.2. Projections Related to Cyclone Classes

Dowdy et al. [2013b] found, using two climate models, that the occurrence of ECLs will decrease with a warming climate. This decrease has been confirmed with high-resolution regional climate simulations [*Ji et al.*, 2015] and with further multimodel studies [*Pepler et al.*, 2016]. However, *Pepler et al.* [2016] find that there may be more ECLs exhibiting heavy precipitation in a future climate.

The future of the serial clustering of cyclones (discussed in section 3.8.3) has been investigated by *Pinto et al.* [2013] and *Economou et al.* [2015]. If all intensities of cyclones are taken into account, there is much disagreement between models and the mean change is small. Considering the extreme cyclones (defined based on percentiles of storm-associated mean sea level pressure at each grid point), there is a projected increase in clustering of these cyclones over Northern Europe and Scandinavia.

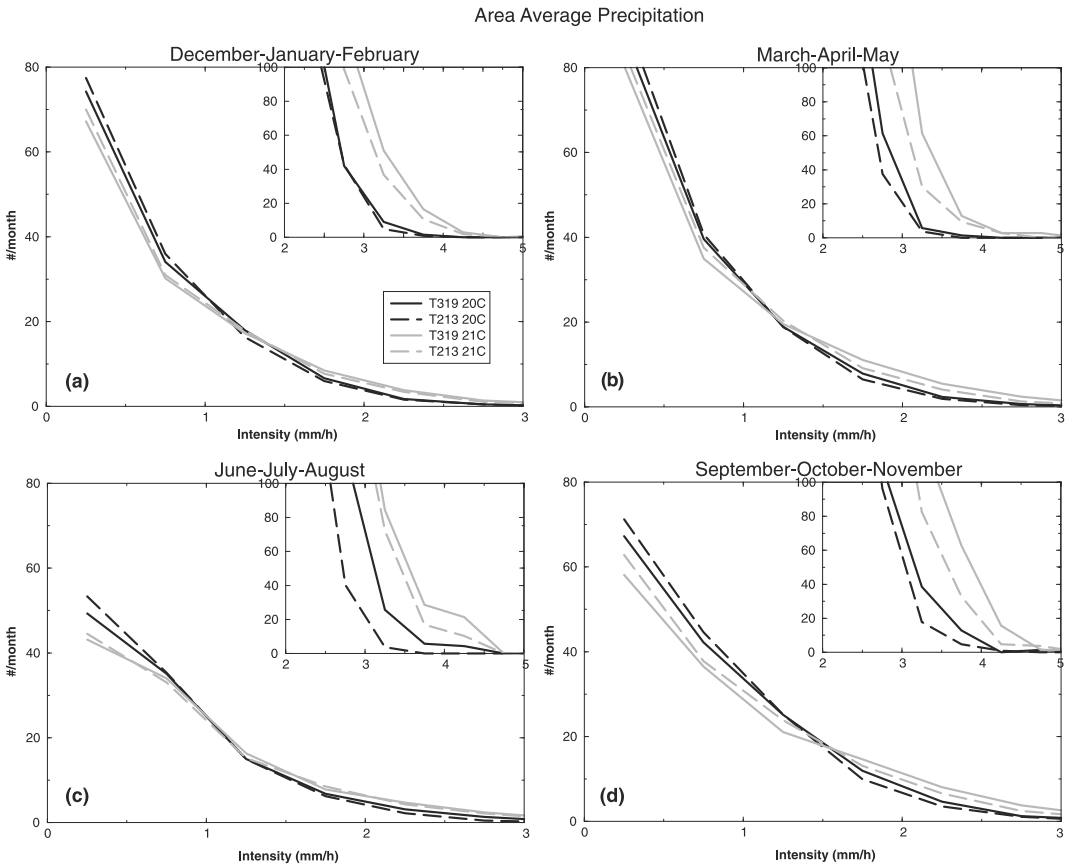

Figure 13. Area average precipitation along the storm track within a 5° area of the storm's center for (a) December–February, (b) March–May, (c) June–August, and (d) September–November. The ECHAM5 T319 resolution is shown by the solid lines, dashed lines are the T213 resolution. The black lines are for the 20th century and the gray lines are for 21st century. The insets are the tails of the distributions scaled to 30 years (90 months). (From *Champion et al.* [2011], licensed under CC BY 4.0 (http://creativecommons.org/licenses/by/4.0/legalcode).)

Associated with increases in the most intense cyclones [e.g., *Feser et al.*, 2015], a number of studies have found increases in windstorm-related losses over Europe in a warmer climate [*Leckebusch et al.*, 2007; *Pinto et al.*, 2012; *Held et al.*, 2013]. A review of literature on future storm damages by *Ranson et al.* [2014]—where the authors attempted to standardize the many differing procedures and remove the influence of population growth on damage estimates—also finds strong evidence for increased losses in the future. Consideration of the location of the high winds within the storm producing the extreme wind events (as in *Hewson and Neu* [2015]) may offer additional insight into these types of future projections.

5.3. Projections of Related Features

Given the coupling of many different classes of cyclones with the upper level jet [e.g., *Evans et al.*, 1994; *Sinclair and Revell*, 2000; *Deveson et al.*, 2002], this is of major importance to changes in the extratropical storm tracks, and the differing classes of cyclones within them. The IPCC AR5 finds that "poleward shifts in the mid-latitude jets of about 1 to 2° latitude are likely at the end of the 21st century under RCP8.5 in both hemispheres (medium confidence), with weaker shifts in the NH" [*Collins et al.*, 2013]. These projected changes, however, are not necessarily zonally symmetric.

One of the mechanisms to which some studies attribute their projected cyclone number reductions is known as "Arctic amplification" [e.g., *Screen and Simmonds*, 2013]. This is the phenomenon whereby the Arctic region warms (and is projected to warm) much more than the midlatitudes (at low levels in the atmosphere). This acts to decrease the meridional temperature gradient, thereby decreasing the baroclinicity. For classes of cyclones with a high dependence on the surface temperature gradient (e.g., Type A from the threefold classification of *Deveson et al.* [2002] or the emerging cloud head from *Evans et al.* [1994]), this would likely decrease the rate of cyclogenesis.

Classification	Feature/Process												
	Diffluent flow	Confluent flow	Weak upper level trough	Sharp trough	Cyclogenesis far from polar front (cold side)	Interaction with polar front	Strong upper level forcing	Weak upper level forcing	Secondary cyclo-genesis	Strong cold front	Strong warm front	Bent back front	Weak front
Threefold classification [*Deveson et al.*, 2002]													
Type A			X			X		X					
Type B				X		X			X				
Type C				X	X		X						X
Satellite classification [*Evans et al.*, 1994]													
Emerging cloud head			X			X							
Left exit	X					X							
Instant occlusion		X				X							
Comma cloud					X		X						
Upper level features [*Sinclair and Revell*, 2000]													
Upstream exit (U)	X				X	X				X			
Downstream exit (D)	X	X				X					X		
Equatorward entrance (E)		X				X							
Trough (T)				X	X							X	
Conceptual Models													
Norwegian	X					X		X		X			
Shapiro-Keyser		X				X					X	X	

Figure 14. Schematic showing some of the features that different classes of cyclones from different classification techniques exhibit. This is not an exhaustive list and the lack of a specific feature being indicated does not necessarily mean that these classes do not exhibit such features. The classifications are the threefold classification of *Deveson et al.* [2002], the satellite cloud classes of *Evans et al.* [1994], the manual classes of *Sinclair and Revell* [2000], and the conceptual life cycle models (Norwegian and Shapiro-Keyser).

As well as the overall projected decrease in baroclinicity in the NH, the underlying SST distribution may also change. The projected slowdown of the AMOC [*Chen et al.*, 2013; *Collins et al.*, 2013] contributes to a localized warming minimum in the North Atlantic. The storm tracks in this region are sensitive to this local change in SSTs [*Catto et al.*, 2011; *Woollings et al.*, 2012]. The location of this SST change could impact on the different classes of cyclones—relative minima in the SST may reduce the potential for strongly diabatically influenced cyclones in this region (such as Type C [*Deveson et al.*, 2002] or the comma cloud formation [*Evans et al.*, 1994]).

Rossby wave breaking (discussed in section 3.1) is projected to change in the future. *Barnes and Hartmann* [2012] investigated projections of this phenomenon in a number of climate models and found that in the SH—where the models show consistent poleward shifts of the jet—cyclonic RWB on the poleward side of the jet decreases in frequency. Anticyclonic RWB, which has its peak frequency on the equatorward side of the jet, shifts poleward with the jet. Since cutoff cyclones are more often associated with anticyclonic RWB [*Thorncroft et al.*, 1993], such a change could influence the location and frequency of upper level cutoff cyclones and thereby the cyclogenesis of certain types of cyclones (e.g., Types B and C from the threefold classification).

6. Conclusions

6.1. Summary

Despite the observation by *Zillman and Price* [1972] that "no two vortices are the same," there has been much research dedicated to the classification of extratropical cyclones. These methods have been used to gain more insight into extratropical cyclone dynamics and to aid in the forecasting of these systems. The methods identified in this review include simple conceptual models, baroclinic life cycles, airflow analysis, satellite classification using cloud signatures, synoptic precursors (e.g., the location of the upper level jet), and dynamical forcing (e.g., the relative forcing from upper or lower levels). Figure 14 shows a diagram indicating the features that some of the classifications detailed in section 3 exhibit. The summary in Figure 14 is not exhaustive, since not all the features mentioned were investigated in each classification study. With the wealth of available satellite data sets, and the availability of higher resolution gridded reanalysis data sets, this information could potentially be expanded.

Extratropical cyclones have huge socioeconomic impacts due to their associated precipitation and strong winds, and these features have also been used to group cyclones. From an observational point of view, more insight could be gained from combining a number of the classification techniques. Studies have shown that

cyclones typically exhibit different characteristics when they occur in different regions. The development of a classification system that encompasses all the different types of cyclones in different regions would be extremely useful in climate model evaluation and the study of potential future climate changes.

There are a number of limitations to the studies performed in the past. Often, they may be subjective, based on data from a limited domain or covering only short time periods. Improvements in atmospheric observing capabilities and data sets, combined with increased computational processing power, will allow the results of previous studies to be expanded using the classification schemes highlighted in Figure 14. Ultimately, doing such classification will provide greater information on extratropical cyclones.

Many studies have evaluated climate model performance in the representation of extratropical cyclones and storm tracks. Although models perform well overall, there are remaining biases in cyclone locations, intensities, cloud features, and precipitation. In particular, moist processes (such as cloud microphysics, convection, and surface fluxes) exhibit biases that can impact on cyclone development and larger-scale climate features, including the tracks of the cyclones [*Coronel et al.*, 2015]. The impacts of the misrepresentation of a number of processes (such as ocean circulation and Arctic amplification) and climate features (such as the jet stream) on these cyclones also need to be taken into account.

Future changes in extratropical cyclones will be sensitive to a number of interacting processes. For example, changes in baroclinicity due to Arctic amplification, increased moisture availability, shifts in the jet position, and associated Rossby wave breaking will all affect the average storm track locations, as well as the cyclone types.

6.2. Improved Observational Capabilities

The information available from satellites has improved considerably in recent decades, thereby allowing more information to be gained about the vertical distribution clouds within extratropical cyclones. The International Satellite Cloud Climatology Project (ISCCP) [*Rossow and Schiffer*, 2001] uses passive sensors to provide gridded data of cloud location and occurrence, sorted into bins according to cloud top pressure and visible optical depth. Cloud profiling radar on CloudSat and the Cloud-Aerosol Lidar with Orthogonal Polarization (CALIOP) on the Cloud-Aerosol Lidar and Infrared Pathfinder Satellite Observations (CALIPSO) satellite can sample the vertical structure of clouds, which has been a great advance for studies of extratropical cyclone cloud features [e.g., *Lau and Crane*, 1995, 1997; *Posselt et al.*, 2008; *Naud et al.*, 2012, 2015; *Booth et al.*, 2013a; *Govekar et al.*, 2014]. Despite this increased information, there have not been any recent attempt to classify cyclones using satellite data; however, these data have been shown to add extra insight to other studies [*Field and Wood*, 2007], such as how cloud and precipitation vary with cyclone strength.

There are a number of reanalysis data sets available that give global data coverage over long time periods (primarily in the satellite era, the last ~30 years), typically with a temporal resolution of 6 h. Such data sets have proved invaluable in the production of climatologies of cyclones and their related features [e.g., *Hodges et al.*, 2011; *Madonna et al.*, 2014a]. They are also often used as the primary data set against which model simulations may be evaluated [e.g., *Catto et al.*, 2010].

Some of the shorter-lived cyclones, especially those that undergo rapid development, may not be captured well by reanalysis data sets with temporal resolution of 6 h. The data set produced during the Year of Tropical Convection (YOTC) ([*Waliser and Moncrieff*, 2007] which includes 3 h, high spatial resolution data), may be a valuable resource; however, longer time periods are necessary than the two years (2008–2010) available. One recommendation from this review is that we should aim for higher temporal resolution data for reanalysis products and climate model output so that rapidly developing cyclones can be better resolved and therefore analyzed.

6.3. Future Directions

The quantification of the links between different cyclone classes (qualitatively shown in Figure 14) could be performed by making use of the wealth of new observational data sets and objective techniques. The criteria specified in the different classifications could then be used to compare observational estimates with climate models automatically and to investigate future changes in extratropical cyclone structure, development, and impacts.

The relative importance of diabatic heating in the cyclone development should be investigated in order to develop an understanding of the impact of errors in moist processes in climate models and the future changes

associated with increased moisture availability. Smaller-scale features tend to interact with moist processes more than larger-scale features, so higher-resolution models will be necessary but not sufficient for representing these particular cyclones. Furthermore, the moist processes, such as cloud microphysics and convection, also need to be represented well. The links between large-scale climate features and extratropical cyclones also need to be captured in climate models in order to have confidence in future projections. Linking the large scale to synoptic scale and mesoscale is another area of study that could benefit from classification techniques.

A wealth of literature exists on the North Atlantic storm track, which provides excellent insight into the processes there. Nevertheless, in order to fully understand the spectrum of cyclone genesis and development, the analyses need to be expanded globally. *Flato et al.* [2013] highlighted the need for better assessment of the SH. Not only are there regions that are severely affected by extratropical cyclones in the SH, the radiation budget and large-scale Southern Ocean temperatures are also impacted by not representing cyclones and their associated cloud correctly [*Trenberth and Fasullo*, 2010; *Bodas-Salcedo et al.*, 2012].

Extratropical cyclones are an important consideration for many modeling groups in the development of their models (storm tracks and cyclones are often evaluated between different model versions [e.g., *Greeves et al.*, 2007]); nevertheless, not all cyclones are the same. Cyclone classification techniques could be usefully employed during the model development phase to investigate the representation of the different types of cyclones. In particular, cyclones that most strongly depend on moist processes such as latent heat release (e.g., Type C cyclones) for their development and which may undergo significant changes in a warmer world, could be evaluated separately.

Making use of the classification techniques detailed in this review could provide the climate modeling, model evaluation, and climate change communities with greater insight into the myriad physical processes occurring in these systems, how they are represented, and how they may change in the future. We could gain greater understanding of the mechanisms by which high-impact weather (such as heavy rainfall) develops and how this relates to larger-scale features, understanding of the interconnection of model processes and their biases, and how extratropical cyclones and their associated impacts may change in the future. Ultimately, this could lead to improved projections of climate change impacts in the midlatitudes and provide greater opportunities for adaptation.

Acknowledgments
I gratefully acknowledge the very helpful comments and suggestions of the Editor and two anonymous reviewers, which improved the manuscript. I would like to express my immense gratitude to Duncan Ackerley for reading and commenting on earlier versions of this review and for the very helpful discussions during the writing process. This work was supported by the Australian Research Council project DE140101305.

References

Abbs, D., S. Aryal, E. Campbell, J. McGregor, K. Nguyen, M. Palmer, T. Rafter, I. Watterson, and B. Bates (2006), Projections of extreme rainfall and cyclones: Final report to the Australian Greenhouse Office, 97 pp., CSIRO Marine and Atmospheric Research, Aspendale, Victoria, Australia. [Available at https://publications.csiro.au/rpr/pub?list=SEA&pid=procite:9f7fb6b5-5433-4685-ac47-f6145c2041e2.]

Ahmadi-Givi, F., G. C. Craig, and R. S. Plant (2004), The dynamics of a midlatitude cyclone with very strong latent-heat release, *Q. J. R. Meteorol. Soc.*, *130*, 295–323, doi:10.1256/qj.02.226.

Anthes, R. A., Y.-H. Kuo, and J. R. Gyakum (1983), Numerical simulations of a case of explosive marine cyclogenesis, *Mon. Weather Rev.*, *111*, 1174–1188.

Archambault, H. M., L. F. Bosart, D. Keyser, and J. M. Cordeira (2013), A climatological analysis of the extratropical flow response to recurving western North Pacific tropical cyclones, *Mon. Weather Rev.*, *141*, 2325–2346, doi:10.1175/MWR-D-12-00257.1.

Atallah, E. H., and L. F. Bosart (2003), The extratropical transition and precipitation distribution of Hurricane Floyd (1999), *Mon. Weather Rev.*, *131*, 1063–1081.

Barnes, E. A., and D. L. Hartmann (2012), Detection of Rossby wave breaking and its response to shifts of the midlatitude jet with climate change, *J. Geophys. Res.*, *117*, D09117, doi:10.1029/2012JD017469.

Béguin, A., O. Martius, M. Sprenger, P. Spichtinger, D. Folini, and H. Wernli (2013), Tropopause level Rossby wave breaking in the Northern Hemisphere: A feature-based validation of the ECHAM5-HAM climate model, *Int. J. Climatol.*, *33*, 3073–3082, doi:10.1002/joc.3631.

Bengtsson, L., K. I. Hodges, and E. Roeckner (2006), Storm tracks and climate change, *J. Clim.*, *19*, 3518–3543.

Bengtsson, L., K. I. Hodges, and N. Keenlyside (2009), Will extra-tropical storms intensify in a warmer climate?, *J. Clim.*, *22*, 2276–2301.

Berry, G., M. J. Reeder, and C. Jakob (2011), A global climatology of atmospheric fronts, *Geophys. Res. Lett.*, *38*, L04809, doi:10.1029/2010GL046451.

Bjerknes, J., and H. Solberg (1922), Life cycle of cyclones and the polar front theory of atmospheric circulation, *Geophys. Publ.*, *3*, 1–18.

Blackmon, M. L., J. M. Wallace, N.-C. Lau, and S. L. Mullen (1977), An observational study of the Northern Hemisphere wintertime circulation, *J. Atmos. Sci.*, *34*, 1040–1053.

Blake, E. S., T. B. Kimberlain, R. J. Berg, J. P. Cangialosi, and J. L. Beven III (2013), Tropical cyclone report: Hurricane Sandy (AL182012), *Tech. Rep.*, Natl. Hurricane Cent., Natl. Oceanic and Atmos. Admin, Miami, Fla. [Available online at http://www.nhc.noaa.gov/data/tcr/AL182012_Sandy.pdf, last accessed on 31st May 2016.]

Blechschmidt, A.-M. (2008), A 2-year climatology of polar low events over the Nordic Seas from satellite remote sensing, *Geophys. Res. Lett.*, *35*, L09815, doi:10.1029/2008GL033706.

Bodas-Salcedo, A., K. D. Williams, P. R. Field, and A. P. Lock (2012), The surface downwelling solar radiation surplus over the Southern Ocean in the Met Office model: The role of midlatitude cyclone clouds, *J. Clim.*, *25*, 7467–7486.

Bony, S., et al. (2015), Clouds, circulation and climate sensitivity, *Nat. Geosci.*, *8*(4), 261–268.

Booth, J. F., L. Thomson, J. Patoux, K. A. Kelly, and S. Dickinson (2010), The signature of the midlatitude tropospheric storm tracks in the surface winds, *J. Clim.*, *23*, 1160–1174, doi:10.1175/2009JCLI3064.1.

Booth, J. F., L. Thomson, J. Patoux, and K. A. Kelly (2012), Sensitivity of midlatitude storm intensification to perturbations in the sea surface temperature near the Gulf Stream, *Mon. Weather Rev.*, *140*, 1241–1256, doi:10.1175/MWR-D-11-00195.1.
Booth, J. F., C. M. Naud, and A. D. Del Genio (2013a), Diagnosing warm frontal cloud formation in a GCM: A novel approach using conditional subsetting, *J. Clim.*, *26*, 5827–5845, doi:10.1175/JCLI-D-12-00637.1.
Booth, J. F., S. Wang, and L. Polvani (2013b), Midlatitude storms in a moister world: Lessons from idealized baroclinic life cycle experiments, *Clim. Dyn.*, *41*, 787–802, doi:10.1007/s00382-012-1472-3.
Booth, J. F., H. Reider, D. E. Lee, and Y. Kushnir (2015), The paths of extratropical cyclones associated with wintertime high wind events in the Northeast United States, *J. Appl. Meteorol. Climatol.*, *54*, 1871–1885.
Born, K., P. Ludwig, and J. G. Pinto (2012), Wind gust estimation for Mid-European winter storms: Towards a probabilistic view, *Tellus*, *64A*, 17471, doi:10.3402/tellusa.v64i0.17471.
Brayshaw, D. J., B. Hoskins, and M. Blackburn (2009), The basic ingredients of the North Atlantic storm track. Part 1: Land-sea contrast and orography, *J. Atmos. Sci.*, *66*, 2429–2558.
Brennan, M. J., and G. M. Lackmann (2005), The influence of incipient latent heat release on the precipitation distribution of the 24–25 January 2000 U.S. East Coast cyclone, *Mon. Weather Rev.*, *133*, 1913–1937.
Browning, K. A. (1986), Conceptual models of precipitation systems, *Weather Forecasting*, *1*, 23–41.
Browning, K. A. (1990), Organization of clouds and precipitation in extratropical cyclones, in *Extratropical Cyclones. The Erik Palmen Memorial Volume*, edited by C. Newton and E. O. Holopainen, pp. 129–154, Am. Meteorol. Soc., Boston, Mass.
Browning, K. A. (1997), The dry intrusion perspective of extra-tropical cyclone development, *Meteorol. Appl.*, *4*, 317–324.
Browning, K. A. (2004), The sting at the end of the tail: Damaging winds associated with extratropical cyclones, *Q. J. R. Meteorol. Soc.*, *130*, 375–399, doi:10.1256/qj.02.143.
Browning, S. A., and I. D. Goodwin (2013), Large-scale influences on the evolution of winter subtropical maritime cyclones affecting Australia's East Coast, *Mon. Weather Rev.*, *141*, 2416–2431, doi:10.1175/MWR-D-12-00312.1.
Browning, K. A., and F. F. Hill (1985), Mesoscale analysis of a polar trough interacting with a polar front, *Q. J. R. Meteorol. Soc.*, *111*, 445–462.
Businger, S. (1985), The synoptic climatology of polar low outbreaks, *Tellus*, *37A*, 419–432.
Campins, J., A. Genovés, A. Jansà, J. A. Guijarro, and C. Ramis (2000), A catalogue and a classification of surface cyclones for the western Mediterranean, *Int. J. Climatol.*, *20*, 969–984.
Carleton, A. M., and D. A. Carpenter (1990), Satellite climatology of polar lows and broad scale climatic associations for the Southern Hemisphere, *Int. J. Climatol.*, *10*, 219–246, doi:10.1002/joc.3370100302.
Carlson, T. N. (1980), Airflow through midlatitude cyclones and the comma cloud pattern, *Mon. Weather Rev.*, *129*, 2205–2225.
Catto, J. L., and S. Pfahl (2013), The importance of fronts for extreme precipitation, *J. Geophys. Res. Atmos.*, *118*, 10,791–10,801, doi:10.1002/jgrd.50852.
Catto, J. L., L. C. Shaffrey, and K. I. Hodges (2010), Can climate models capture the structure of extratropical cyclones?, *J. Clim.*, *23*, 1621–1635.
Catto, J. L., L. C. Shaffrey, and K. I. Hodges (2011), Northern Hemisphere extratropical cyclones in a warming climate in the HiGEM high-resolution climate model, *J. Clim.*, *24*, 5336–5352, doi:10.1175/2011JCLI4181.1.
Catto, J. L., C. Jakob, G. Berry, and N. Nicholls (2012), Relating global precipitation to atmospheric fronts, *Geophys. Res. Lett.*, *39*, L10805, doi:10.1029/2012GL051736.
Catto, J. L., E. Madonna, H. Joos, I. Rudeva, and I. Simmonds (2015a), Global relationship between fronts and warm conveyor belts and the impact on extreme precipitation, *J. Clim.*, *28*, 8411–8429, doi:10.1175/JCLI-D-15-0171.1.
Catto, J. L., C. Jakob, and N. Nicholls (2015b), Can the CMIP5 models represent winter frontal precipitation?, *Geophys. Res. Lett.*, *42*, 8596–8604, doi:10.1002/2015GL066015.
Chambers, C. R. S., G. B. Brassington, I. Simmonds, and K. Walsh (2014), Precipitation changes due to the introduction of eddy-resolved sea surface temperatures into simulations of the "Pasha Bulker" east coast low of June 2007, *Meteorol. Atmos. Phys.*, *125*, 1–15, doi:10.1007/s00703-014-0318-4.
Champion, A. J., K. I. Hodges, L. O. Bengtsson, N. S. Keenlyside, and M. Esch (2011), Impact of increasing resolution and a warmer climate on extreme weather from Northern Hemisphere extratropical cyclones, *Tellus*, *63A*, 893–906.
Chang, E. K. M., and S. Song (2006), The seasonal cycles in the distribution of precipitation around cyclones in the Western North Pacific and Atlantic, *J. Atmos. Sci.*, *63*, 815–839.
Chang, E. K. M., S. Lee, and K. L. Swanson (2002), Storm track dynamics, *J. Clim.*, *15*, 2163–2183.
Charney, J. G. (1947), The dynamics of long waves in a baroclinic westerly current, *J. Meteorol.*, *4*, 135–163.
Chen, S.-J., Y.-H. Kuo, P.-Z. Zhang, and Q.-F. Bai (1992), Climatology of explosive cyclones off the east Asian coast, *Mon. Weather Rev.*, *120*, 3029–3035.
Chen, S.-J., Y.-H. Kuo, P.-Z. Zhang, and Q.-F. Bai (2013), Atlantic Meridional Overturning Circulation (AMOC) in CMIP5 models: RCP and historical simulations, *J. Clim.*, *26*, 7189–7197.
Clough, S. A., H. W. Lean, N. W. Roberts, H. Birkett, J.-P. Chaboureau, R. Dixon, M. Griffiths, T. D. Hewson, and A. Montani (1998), 'A JCMM overview of FASTEX IOPSs', *JCMM Internal Rep. 81*, Available from the National Meteorological Library, Exeter, U. K.
Colle, B. A., Z. Zhang, K. A. Lombardo, E. Chang, P. Liu, and M. Zhang (2013), Historical evaluation and future prediction of Eastern North American and Western Atlantic extratropical cyclones in the CMIP5 models during the cool season, *J. Clim.*, *26*, 6882–6903, doi:10.1175/JCLI-D-12-00498.1.
Colle, B. A., J. F. Booth, and E. K. M. Chang (2015), A review of historical and future changes of extratropical cyclones and associated impacts along the US East Coast, *Curr. Clim. Change Rep.*, *1*, 125–143, doi:10.1007/s40641-015-0013-7.
Collins, M., et al. (2013), Long-term climate change: Projections, commitments and irreversibility, in *Climate Change 2013: The Physical Science Basis. Contribution of Working Group I to the Fifth Assessment Report of the Intergovernmental Panel on Climate Change*, chap. 12, edited by T. Stocker et al., pp. 1029–1136, Cambridge Univ. Press, Cambridge, U. K., and New York, doi:10.1017/CBO9781107415324.024.
Coronel, B., D. Ricard, G. Rivière, and P. Arbogast (2015), Role of moist processes in the tracks of idealized midlatitude surface cyclones, *J. Atmos. Sci.*, *72*, 2979–2996, doi:10.1175/JAS-D-14-0337.1.
Dacre, H. F., and S. L. Gray (2009), The spatial distribution and evolution characteristics of North Atlantic cyclones, *Mon. Weather Rev.*, *137*, 99–115.
Dacre, H. F., and S. L. Gray (2013), Quantifying the climatological relationship between extratropical cyclone intensity and atmospheric precursors, *Geophys. Res. Lett.*, *40*, 2322–2327, doi:10.1002/grl.50105.
Dacre, H. F., P. A. Clark, O. Martinez-Alvarado, M. A. Stringer, and D. A. Lavers (2015), How do atmospheric rivers form?, *Bull. Am. Meteorol. Soc.*, *96*, 1243–1255, doi:10.1175/bams-d-14-00031.1.
Dai, A., and T. M. L. Wigley (2000), Global patterns of ENSO-induced precipitation, *Geophys. Res. Lett.*, *9*, 1283–1286.

Davies, H. C., C. Schär, and H. Wernli (1991), The palette of fronts and cyclones within a baroclinic wave development, *J. Atmos. Sci.*, *48*, 1666–16,898.
Davis, C. A. (2010), Simulations of subtropical cyclones in a baroclinic channel model, *J. Atmos. Sci.*, *67*, 2871–2892, doi:10.1175/2010JAS3411.1.
Davis, C. A., and K. A. Emanuel (1988), Observational evidence for the influence of surface heat fluxes on rapid maritime cyclogenesis, *Mon. Weather Rev.*, *116*, 2649–2659.
Davis, C. A., and K. A. Emanuel (1991), Potential vorticity diagnostics of cyclogenesis, *Mon. Weather Rev.*, *119*, 1929–1953.
Dee, D. P., et al. (2011), The ERA-Interim reanalysis: Configuration and performance of the data assimilation system, *Q. J. R. Meteorol. Soc.*, *137*, 553–597.
Deveson, A. C. L., K. A. Browning, and T. D. Hewson (2002), A classification of FASTEX cyclones using a height-attributable quasi-geostrophic vertical-motion diagnostic, *Q. J. R. Meteorol. Soc.*, *128*, 93–117.
DiMego, G. J., and L. F. Bosart (1982), The transformation of tropical storm Agnes into an extratropical cyclones. Part I: The observed fields and vertical motion computation, *Mon. Weather Rev.*, *110*, 385–411.
Dowdy, A. J., G. A. Mills, and B. Timbal (2013a), Large-scale diagnostics of extratropical cyclogenesis in eastern Australia, *Int. J. Climatol.*, *33*, 2318–2327, doi:10.1002/joc.3599.
Dowdy, A. J., G. A. Mills, B. Timbal, and Y. Wang (2013b), Changes in the risk of extratropical cyclones in Eastern Australia, *J. Clim.*, *26*, 1403–1417, doi:10.1175/jcli-d-12-00192.1.
Eady, E. T. (1949), Long waves and cyclone waves, *Tellus*, *1*, 33–52, doi:10.1111/j.2153-3490.1949.tb01265.x.
Eckhardt, S., A. Stohl, H. Wernli, P. James, C. Forster, and N. Spichtinger (2004), A 15-year climatology of warm conveyor belts, *J. Clim.*, *17*, 218–237.
Economou, T., D. B. Stephenson, J. G. Pinto, L. C. Shaffrey, and G. Zappa (2015), Serial clustering of extratropical cyclones in a multi-model ensemble of historical and future simulations, *Q. J. R. Meteorol. Soc.*, *141*, 3076–3087, doi:10.1002/qj.2591.
Eichler, T., and W. Higgins (2006), Climatology and ENSO-related variability of North American extratropical cyclone activity, *J. Clim.*, *19*, 2076–2093.
Elsberry, R. L., and P. J. Kirchoffer (1988), Upper-level forcing of explosive cyclogenesis over the ocean based on operationally analyzed fields, *Weather Forecasting*, *3*, 205–216.
Emanuel, K. A., and R. Rotunno (1989), Polar lows as arctic hurricanes, *Tellus*, *41A*, 1–17.
Emanuel, K. A., M. Fantini, and A. J. Thorpe (1987), Baroclinic instability in an environment of small stability to slantwise moist convection. Part I: Two-dimensional models, *J. Atmos. Sci.*, *44*, 1559–1573.
Evans, C., and R. E. Hart (2008), Analysis of the wind field evolution associated with the extratropical transition of Bonnie (1998), *Mon. Weather Rev.*, *136*(6), 2047–2065, doi:10.1175/2007MWR2051.1.
Evans, J. L., and M. P. Guishard (2009), Atlantic subtropical storms. Part I: Diagnostic criteria and composite analysis, *Mon. Weather Rev.*, *137*, 2065–2080.
Evans, M. S., D. Keyser, L. F. Bosart, and G. M. Lackmann (1994), A satellite-derived classification scheme for rapid maritime cyclogenesis, *Mon. Weather Rev.*, *122*, 1381–1416.
Fantini, M. (2004), Baroclinic instability of a zero-PVE jet: Enhanced effects of moisture on the life cycle of midlatitude cyclones, *J. Atmos. Sci.*, *61*, 1663–1680.
Feser, F., M. Barcikowska, O. Krueger, F. Schenk, R. Weisse, and L. Xia (2015), Storminess over the North Atlantic and northwestern Europe—A review, *Q. J. R. Meteorol. Soc.*, *141*, 350–382, doi:10.1002/qj.2364.
Field, P. R., and R. Wood (2007), Precipitation and cloud structure in midlatitude cyclones, *J. Clim.*, *20*, 233–254.
Field, P. R., A. Gettelman, R. Neale, R. Wood, P. J. Rasch, and H. Morrison (2008), Midlatitude cyclone compositing to constrain climate model behavior using satellite observations, *J. Clim.*, *21*, 5887–5903.
Fink, A. H., T. Brücher, V. Ermert, A. Krüger, and J. G. Pinto (2009), The European storm Kyrill in January 2007: Synoptic evolution, meteorological impacts and some considerations with respect to climate change, *Natl. Hazards Earth Syst. Sci.*, *9*, 405–423.
Fink, A. H., S. Pohle, J. G. Pinto, and P. Knippertz (2012), Diagnosing the influence of diabatic processes on the explosive deepening of extratropical cyclones, *Geophys. Res. Lett.*, *39*, L07803, doi:10.1029/2012GL051025.
Fita, L., R. Romero, and C. Ramis (2006), Intercomparison of intense cyclogenesis events over the Mediterranean basin based on baroclinic and diabatic influences, *Ann. Geophys.*, *7*, 333–342.
Flato, G., et al. (2013), Evaluation of climate models, in *Climate Change 2013: The Physical Science Basis. Contribution of Working Group I to the Fifth Assessment Report of the Intergovernmental Panel on Climate Change*, edited by T. Stocker et al., Cambridge Univ. Press, Cambridge, U. K., and New York, doi:10.1017/CBO9781107415324.020.
Flocas, H. A., I. Simmonds, J. Kouroutzoglou, K. Keay, M. Hatzaki, V. Bricolas, and D. Asimakopoulos (2010), On cyclonic tracks over the eastern Mediterranean, *J. Clim.*, *23*(19), 5243–5257, doi:10.1175/2010JCLI3426.1.
Forbes, G. S., and W. D. Lottes (1985), Classification of mesoscale vortices in polar airstreams and the influence of the large-scale environment on their evolutions, *Tellus*, *37A*, 132–155.
Galarneau, T. J., Jr., C. A. Davis, and M. A. Shapiro (2013), Intensification of hurricane Sandy (2012) through extratropical warm core seclusion, *Mon. Weather Rev.*, *141*, 4296–4321, doi:10.1175/MWR-D-13-00181.1.
Gillett, N. P., T. D. Kell, and P. D. Jones (2006), Regional climate impacts of the Southern Annular Mode, *Geophys. Res. Lett.*, *33*, L23704, doi:10.1029/2006GL027721.
Gómara, I., J. Pinto, G. Masato, P. Zurita-Gotor, and B. Rodríguez-Fonseca (2014), Rossby wave-breaking analysis of explosive cyclones in the Euro-Atlantic sector, *Q. J. R. Meteorol. Soc.*, *140*, 738–753, doi:10.1002/qj.2190.
Govekar, P., C. Jakob, M. J. Reeder, and J. Haynes (2011), The three-dimensional distribution of clouds around Southern Hemisphere extratropical cyclones, *Geophys. Res. Lett.*, *38*, L21805, doi:10.1029/2011GL049091.
Govekar, P., C. Jakob, and J. L. Catto (2014), The relationship between clouds and dynamics in Southern Hemisphere extratropical cyclones in the real world and a climate model, *J. Geophys. Res. Atmos.*, *119*, 6609–6628, doi:10.1002/2013JD020699.
Graf, M. A. (2014), Objektive klassifikation von zyklogenese in den aussertropen, PhD thesis, ETH Zürich, Zurich, Switzerland, doi:10.3929/ethz-a-010198550.
Grams, C. M., S. C. Jones, C. A. Davis, P. A. Harr, and M. Weissmann (2013a), The impact of typhoon Jangmi(2008) on the midlatitude flow. Part I: Upper-level ridge building and modification of the jet, *Q. J. R. Meteorol. Soc.*, *139*, 2148–2164, doi:10.1002/qj.2091.
Grams, C. M., S. C. Jones, and C. A. Davis (2013b), The impact of typhoon Jangmi (2008) on the midlatitude flow. Part II: Downstream evolution, *Q. J. R. Meteorol. Soc.*, *139*, 2165–2180, doi:10.1002/qj.2119.
Gray, S. L., and H. F. Dacre (2006), Classifying dynamical forcing mechanisms using a climatology of extratropical cyclones, *Q. J. R. Meteorol. Soc.*, *132*, 1119–1137.

Greeves, C. Z., V. D. Pope, R. A. Stratton, and G. M. Martin (2007), Representation of Northern Hemisphere winter storm tracks in climate models, *Clim. Dyn.*, *28*, 683–702, doi:10.1007/s00382-006-0205-x.
Grønås, S., and N. G. Kvamstø (1995), Numerical simulations of the synoptic conditions and development of Arctic outbreak polar lows, *Tellus*, *47A*, 797–814.
Guishard, M. P., J. L. Evans, and R. E. Hart (2009), Atlantic subtropical storms. Part II: Climatology, *J. Clim.*, *22*, 3574–3594.
Gyakum, J. R., et al. (1996), A regional model intercomparison using a case of explosive oceanic cyclogenesis, *Weather Forecasting*, *11*, 521–543.
Haas, R., and J. G. Pinto (2012), A combined statistical and dynamical approach for downscaling large-scale footprints of European windstorms, *Geophys. Res. Lett.*, *39*, L23804, doi:10.1029/2012GL054014.
Hadlock, R., and C. W. Kreitzberg (1988), The Experiment on Rapidly Intensifying Cyclones Over the Atlantic (ERICA) field study: Objectives and plans, *Bull. Am. Meteorol. Soc.*, *69*, 1309–1320.
Harrold, T. W. (1973), Mechanisms influencing the distribution of precipitation within baroclinic disturbances, *Q. J. R. Meteorol. Soc.*, *99*, 232–251.
Hart, R. E. (2003), A cyclone phase space derived from thermal wind and thermal asymmetry, *Mon. Weather Rev.*, *131*, 585–616.
Hart, R. E., and J. L. Evans (2001), A climatology of extratropical transition of Atlantic tropical cyclones, *J. Clim.*, *14*, 546–564.
Hawcroft, M. K., L. C. Shaffrey, K. I. Hodges, and H. F. Dacre (2012), How much Northern Hemisphere precipitation is associated with extratropical cyclones?, *Geophys. Res. Lett.*, *39*, L24809, doi:10.1029/2012GL053866.
Hawcroft, M. K., L. C. Shaffrey, K. I. Hodges, and H. F. Dacre (2015), Can climate models represent the precipitation associated with extratropical cyclones?, *Clim. Dyn.*, 1–17, doi:10.1007/s00382-015-2863-z.
Held, H., et al. (2013), Projections of global warming-induced impacts on winter storm losses in the German private household sector, *Clim. Change*, *121*, 195–207.
Heo, K.-Y., Y.-W. Seo, K.-J. Ha, K.-S. Park, J. Kima, J.-W. Choia, K. Juna, and J.-Y. Jeonga (2015), Development mechanisms of an explosive cyclone over East Sea on 3–4 April 2012, *Dyn. Atmos. Oceans*, *70*, 30–46.
Hewson, T. D. (1998), Objective fronts, *Meteorol. Appl.*, *5*, 37–65.
Hewson, T. D., and U. Neu (2015), Cyclones, windstorms and the IMILAST project, *Tellus A*, *67A*, 27128, doi:10.3402/tellusa.v67.27128.
Hewson, T. D., and H. A. Titley (2010), Objective identification, typing and tracking of the complete life-cycles of cyclonic features at high spatial resolution, *Meteorol. Appl.*, *17*, 355–381, doi:10.1002/met.204.
Hirata, H., R. Kawamura, M. Kato, and T. Shinoda (2015), Influential role of moisture supply from the Kuroshio/Kuroshio extension in the rapid development of an extratropical cyclone, *Mon. Weather Rev.*, *143*, 4126–4144, doi:10.1175/MWR-D-15-0016.1.
Hodges, K. I. (2008), Confidence intervals and significance tests for spherical data derived from feature tracking, *Mon. Weather Rev.*, *136*, 1758–1777.
Hodges, K. I., R. W. Lee, and L. Bengtsson (2011), A comparison of extratropical cyclones in recent reanalyses ERA-Interim, NASA, MERRA, NCEP CFSR, and JRA-25, *J. Clim.*, *24*, 4888–4906.
Holland, G. J., A. H. Lynch, and L. M. Leslie (1987), Australian east-coast cyclones. Part I: Synoptic overview and case study, *Mon. Weather Rev.*, *115*, 3024–3036.
Hopkins, L. C., and G. J. Holland (1997), Australian heavy-rain days and associated east coast cyclones: 1958–92, *J. Clim.*, *10*, 621–635.
Hoskins, B. J. (1976), Baroclinic waves and frontogenesis, Part I: Introduction and Eady waves, *Q. J. R. Meteorol. Soc.*, *102*, 103–122, doi:10.1002/qj.49710243109.
Hoskins, B. J. (1981), Cold and warm fronts in a baroclinic wave, *Q. J. R. Meteorol. Soc.*, *107*, 79–90.
Hoskins, B. J., and P. Berrisford (1988), A potential vorticity perspective of the storm of 15–16 October 1987, *Weather*, *43*, 122–129, doi:10.1002/j.1477-8696.1988.tb03890.x.
Hoskins, B. J., and P. J. Valdes (1990), On the existence of storm tracks, *J. Atmos. Sci.*, *47*, 1854–1864, doi:10.1175/1520-0469(1990)047<1854:OTEOST>2.0.CO;2.
Hoskins, B. J., and N. V. West (1979), Baroclinic waves and frontogenesis. Part II: Uniform potential vorticity jet flows—Cold and warm fronts, *J. Atmos. Sci.*, *36*, 1663–1680.
Hoskins, B. J., M. E. McIntyre, and A. W. Robertson (1985), On the use and significance of isentropic potential vorticity maps, *Q. J. R. Meteorol. Soc.*, *111*, 877–946.
Irvine, E. A., S. L. Gray, J. Methven, I. A. Renfrew, K. Bovis, and R. Swinbank (2011), The impact of targeted observations made during the Greenland Flow Distortion Experiment, *Q. J. R. Meteorol. Soc.*, *135*, 2012–2029, doi:10.1002/qj.499.
Ji, F., J. P. Evans, D. Argueso, L. Fita, and A. Di Luca (2015), Using large-scale diagnostic quantities to investigate change in East Coast Lows, *Clim. Dyn.*, *45*, 2443–2453, doi:10.1007/s00382-015-2481-9.
Joly, A., et al. (1997), The Fronts and Atlantic Storm-Track EXperiment (FASTEX): Scientific objectives and experimental design, *Bull. Am. Meteorol. Soc.*, *78*, 1917–1940.
Joly, A., et al. (1999), Overview of the field phase of the Fronts and Atlantic Storm-Track Experiment (FASTEX) project, *Q. J. R. Meteorol. Soc.*, *125*, 3131–3163.
Jones, S. C., et al. (2003), The extratropical transition of tropical cyclones: Forecast challenges, current understanding, and future directions, *Weather Forecasting*, *18*, 1052–1092.
Joos, H., and H. Wernli (2012), Influence of microphysical processes on the potential vorticity development in a warm conveyor belt: A case-study with the limited-area model COSMO, *Q. J. R. Meteorol. Soc.*, *138*, 407–418.
Jung, T., S. K. Gulev, I. Rudeva, and V. Soloviov (2006), Sensitivity of extratropical cyclone characteristics to horizontal resolution in the ECMWF model, *Q. J. R. Meteorol. Soc.*, *132*, 1839–1857.
Junker, N. W., and D. J. Haller (1980), Estimation of surface pressures from satellite cloud patterns, *Mar. Weather Log.*, *24*, 83–87.
Keeley, S. P. E., R. T. Sutton, and L. C. Shaffrey (2012), The impact of North Atlantic sea surface temperature errors on the simulation of North Atlantic European region climate, *Q. J. R. Meteorol. Soc.*, *138*, 1774–1783.
Keyser, D., B. D. Schmidt, and D. G. Duffy (1989), A technique for representing three-dimensional vertical circulations in baroclinic disturbances, *Mon. Weather Rev.*, *117*, 2463–2494.
Kirtman, B., et al. (2013), Near-term climate change: Projections and predictability, in *Climate Change 2013: The Physical Science Basis. Contribution of Working Group I to the Fifth Assessment Report of the Intergovernmental Panel on Climate Change*, chap. 11, edited by T. Stocker et al., pp. 953–1028, Cambridge Univ. Press, Cambridge, U. K., and New York, doi:10.1017/CBO9781107415324.023.
Klawa, M., and U. Ulbrich (2003), A model for the estimation of storm losses and the identification of severe winter storms in Germany, *Nat. Hazards Earth Syst. Sci.*, *3*, 725–732.
Klein, P. M., P. A. Harr, and R. L. Elsberry (2000), Extratropical transition of western North Pacific tropical cyclones: An overview and conceptual model of the transformation stage, *Weather Forecasting*, *15*, 373–396.

Kouroutzoglou, J., H. A. Flocas, M. Hatzaki, K. Keay, I. Simmonds, and A. Mavroudis (2015), On the dynamics of a case study of explosive cyclogenesis in the Mediterranean, *Meteorol. Atmos. Phys.*, *127*, 49–73, doi:10.1007/s00703-014-0357-x.
Kumar, D., V. Mishra, and A. R. Ganguly (2014), Evaluating wind extremes in CMIP5 climate models, *Clim. Dyn.*, *45*(1), 441–453, doi:10.1007/s00382-014-2306-2.
Kunkel, K. E., D. R. Easterling, D. A. R. Kristovich, B. Gleason, L. Stoecker, and R. Smith (2012), Meteorological causes of the secular variations in observed extreme precipitation events for the conterminous United States, *J. Hydrometeorol.*, *13*, 1131–1141.
Kuo, Y.-H., M. A. Shapiro, and E. G. Donall (1991), The interaction between baroclinic and diabatic processes in a numerical simulation of a rapidly intensifying extratropical marine cyclone, *Mon. Weather Rev.*, *119*, 368–384.
Langenbrunner, B., and J. D. Neelin (2013), Analyzing ENSO teleconnections in CMIP models as a measure of model fidelity in simulating precipitation, *J. Clim.*, *26*, 4431–4446, doi:10.1175/JCLI-D-12-00542.1.
Lau, N. C., and M. W. Crane (1995), A satellite view of the synoptic-scale organization of cloud properties in midlatitude and tropical circulation systems, *Mon. Weather Rev.*, *123*, 1984–2006.
Lau, N. C., and M. W. Crane (1997), Comparing satellite and surface observations of cloud patterns in synoptic-scale circulation systems, *Mon. Weather Rev.*, *125*, 3172–3189.
Lavers, D. A., R. P. Allan, E. F. Wood, G. Villarini, D. J. Brayshaw, and A. J. Wade (2011), Winter floods in Britain are connected to atmospheric rivers, *Geophys. Res. Lett.*, *38*, L23803, doi:10.1029/2011GL049783.
Leckebusch, G. C., B. Koffi, U. Ulbrich, J. G. Pinto, T. Spangehl, and S. Zacharias (2006), Analysis of frequency and intensity of European winter storm events from a multi-model perspective at synoptic and regional scales, *Clim. Res.*, *31*, 59–74.
Leckebusch, G. C., U. Ulbrich, L. Frölich, and J. G. Pinto (2007), Property loss potentials for European midlatitude storms in a changing climate, *Geophys. Res. Lett.*, *34*, L05703, doi:10.1029/2006GL027663.
Leckebusch, G. C., R. Renggli, and U. Ulbrich (2008), Development and application of an objective storm severity measure for the Northeast Atlantic region, *Meteorol. Z.*, *17*, 575–587, doi:10.1127/0941-2948/2008/0323.
Lee, Y.-Y., and R. X. Black (2013), Boreal winter low-frequency variability in CMIP5 models, *J. Geophys. Res. Atmos.*, *118*, 6891–6904, doi:10.1002/jgrd.50493.
Leslie, L. M., G. J. Holland, and A. H. Lynch (1987), Australian East-Coast cyclones. Part II: Numerical modeling study, *Mon. Weather Rev.*, *115*, 3037–3053.
Liberato, M. R. L., J. G. Pinto, I. F. Trigo, and R. M. Trigo (2011), Klaus—An exceptional winter storm over northern Iberia and southern France, *Weather*, *66*, 330–334, doi:10.1002/wea.755.
Lim, E.-P., and I. Simmonds (2002), Explosive cyclone development in the Southern Hemisphere and a comparison with Northern Hemisphere events, *Mon. Weather Rev.*, *130*, 2188–2209.
Lindzen, R. S., and B. Farrell (1980), A simple approximate result for the maximum growth rate of baroclinic instabilities, *J. Atmos. Sci.*, *37*, 1648–1654.
Löptien, U., O. Zolina, S. Gulev, M. Latif, and V. Soloviov (2008), Cyclone life cycle characteristics over the Northern Hemisphere in coupled GCMs, *Clim. Dyn.*, *31*(5), 507–532.
Ludwig, P., J. G. Pinto, M. Reyers, and S. L. Gray (2014), The role of anomalous SST and surface fluxes over the southeastern North Atlantic in the explosive development of windstorm Xynthia, *Q. J. R. Meteorol. Soc.*, *140*, 1729–1741.
Madonna, E., H. Wernli, H. Joos, and O. Martius (2014a), Warm conveyor belts in the ERA-Interim dataset (1979–2010). Part I: Climatology and potential vorticity evolution, *J. Clim.*, *27*, 3–26, doi:10.1175/JCLI-D-12-00720.1.
Madonna, E., S. Limbic, C. Aebi, H. Joos, H. Wernli, and O. Martius (2014b), On the co-occurrence of warm conveyor belt outflows and PV streamers, *J. Atmos. Sci.*, *71*, 3668–3673, doi:10.1175/JAS-D-14-0119.1.
Maheras, P., H. Flocas, I. Patrikas, and C. Anagnostopoulou (2001), A 40 year objective climatology of surface cyclones in the Mediterranean region: Spatial and temporal distribution, *Int. J. Climatol.*, *21*(1), 109–130, doi:10.1002/joc.599.
Mailier, P. J., D. B. Stephenson, C. A. T. Ferro, and K. I. Hodges (2006), Serial clustering of extratropical cyclones, *Mon. Weather Rev.*, *134*, 2224–2240.
Manobianco, J. (1989), Explosive east coast cyclogenesis over the west-central North Atlantic Ocean: A composite study derived from ECMWF operational analyses, *Mon. Weather Rev.*, *117*, 2365–2383.
Martinez-Alvarado, O., S. L. Gray, J. L. Catto, and P. A. Clark (2012), Sting jets in intense winter North-Atlantic windstorms, *Environ. Res. Lett.*, *7*, 24014, doi:10.1088/1748-9326/7/2/024014.
Martius, O., C. Schwierz, and H. C. Davies (2007), Breaking waves at the tropopause in the wintertime Northern Hemisphere: Climatological analyses of the orientation and the theoretical LC1/2 classification, *J. Atmos. Sci.*, *64*, 2576–2592.
Martius, O., C. Schwierz, and M. Sprenger (2008), Dynamical tropopause variability and potential vorticity streamers in the Northern Hemisphere—A climatological analysis, *Adv. Atmos. Sci.*, *25*, 367–379.
Masato, G., B. J. Hoskins, and T. Woollings (2013a), Wave-breaking characteristics of Northern Hemisphere winter blocking: A two-dimensional approach, *J. Clim.*, *26*, 4535–4549, doi:10.1175/jcli-d-12-00240.1.
Masato, G., B. J. Hoskins, and T. Woollings (2013b), Winter and summer Northern Hemisphere blocking in CMIP5 models, *J. Clim.*, *26*, 7044–7059, doi:10.1175/jcli-d-12-00466.1.
McTaggart-Cowan, R., L. F. Bosart, C. A. Davis, E. H. Atallah, J. R. Gyakum, and K. A. Emanuel (2006), Analysis of Hurricane Catarina (2004), *Mon. Weather Rev.*, *134*(11), 3029–3053, doi:10.1175/MWR3330.1.
Michel, C., G. Rivière, L. Terray, and B. Joly (2012), The dynamical link between surface cyclones, upper-tropospheric Rossby wave breaking and the life cycle of the Scandinavian blocking, *Geophys. Res. Lett.*, *39*, L10806, doi:10.1029/2012GL051682.
Mills, G. A. (2001), Mesoscale cyclogenesis in reversed shear—The 1998 Sydney to Hobart yacht race storm, *Aust. Meteorol. Mag.*, *50*, 29–52.
Mills, G. A., R. Webb, N. E. Davidson, J. Kepert, A. Seed, and D. Abbs (2010), The Pasha Bulker east coast low of 8 June 2007, Tech. Rep. 23, Centre for Australia Weather and Climate Research. [Available at available at http://www.cawcr.gov.au/technical-reports/CTR_023.pdf.]
Mullen, S. L. (1983), Explosive cyclogenesis associated with cyclones in polar air streams, *Mon. Weather Rev.*, *111*, 1537–1553.
Nakamura, H. (1992), Midwinter suppression of baroclinic wave activity in the Pacific, *J. Atmos. Sci.*, *49*, 1629–1642.
Naud, C. M., A. D. Del Genio, M. Bauer, and W. Kovari (2010), Cloud vertical distribution across warm fronts in CloudSat-CALIPSO data and a general circulation model, *J. Clim.*, *23*, 3397–3415, doi:10.1175/ 2010JCLI3282.1.
Naud, C. M., D. J. Posselt, and S. C. van den Heever (2012), Observational analysis of cloud and precipitation in midlatitude cyclones: Northern versus Southern Hemisphere warm fronts, *J. Clim.*, *25*, 5135–5151.
Naud, C. M., D. J. Posselt, and S. C. van den Heever (2015), A CloudSat-CALIPSO view of cloud and precipitation properties across cold fronts over the global oceans, *J. Clim.*, *28*, 6743–6762, doi:10.1175/JCLI-D-15-0052.1.
Neiman, P. J., and M. A. Shapiro (1993), The life cycle of an extratropical marine cyclone. Part I: Frontal-cyclone evolution and thermodynamic air-sea interaction, *Mon. Weather Rev.*, *121*, 2153–2176.

Neiman, P. J., M. A. Shapiro, and L. S. Fedor (1993), The life cycle of an extratropical marine cyclone. Part II: Mesoscale structure and diagnostics, *Mon. Weather Rev.*, *121*, 2177–2199.
Neu, U., et al. (2013), IMILAST: A community effort to intercompare extratropical cyclone detection and tracking algorithms, *Bull. Am. Meteorol. Soc.*, *94*, 529–547.
Nissen, K. M., G. C. Leckebusch, J. G. Pinto, D. Renggli, S. Ulbrich, and U. Ulbrich (2010), Cyclones causing wind storms in the Mediterranean: Characteristics, trends and links to large-scale patterns, *Nat. Hazards Earth Syst. Sci.*, *10*, 1379–1391, doi:10.5194/nhess-10-1379-2010.
Noer, G., Ø. Saetra, T. Lien, and Y. Gusdal (2011), A climatological study of polar lows in the Nordic Seas, *Q. J. R. Meteorol. Soc.*, *137*, 1762–1772, doi:10.1002/qj.846.
Nordeng, T. E. (1987), The effect of vertical and slantwise convection on the simulation of polar lows, *Tellus*, *39A*, 354–375.
Otkin, J. A., and J. E. Martin (2004), A synoptic climatology of the subtropical Kona storm, *Mon. Weather Rev.*, *132*, 1502–1517.
O'Gorman, P. A., and T. Schneider (2008), Energy of midlatitude transient eddies in idealized simulations of changed climates, *J. Clim.*, *21*(22), 5797–5806, doi:10.1175/2008JCLI2099.1.
Parker, D. J. (1998), Secondary frontal waves in the North Atlantic region: A dynamical perspective of current ideas, *Q. J. R. Meteorol. Soc.*, *124*, 829–856.
Penny, S., G. H. Roe, and D. S. Battisti (2009), The source of midwinter suppression in storminess over the North Pacific, *J. Clim.*, *23*, 634–648.
Pepler, A. S., and A. Coutts-Smith (2013), A new, objective, database of East Coast Lows, *Aust. Meteorol. Ocean J.*, *63*, 461–472.
Pepler, A. S., A. Di Luca, F. Ji, L. V. Alexander, J. P. Evans, and S. C. Sherwood (2015), Impact of identification method on the inferred characteristics and variability of Australian east coast lows, *Mon. Weather Rev.*, *143*, 864–877, doi:10.1175/mwr-d-14-00188.1.
Pepler, A. S., A. Di Luca, F. Ji, L. V. Alexander, J. P. Evans, and S. C. Sherwood (2016), Projected changes in east Australian midlatitude cyclones during the 21st century, *Geophys. Res. Lett.*, *43*, 334–340, doi:10.1002/2015GL067267.
Perlwitz, J. (2011), Atmospheric science: Tug of war on the jet stream, *Nat. Clim. Change*, *1*, 29–31, doi:10.1038/nclimate1065.
Petterssen, S., and S. J. Smebye (1971), On the development of extratropical cyclones, *Q. J. R. Meteorol. Soc.*, *97*, 457–482.
Petterssen, S., D. L. Bradbury, and K. Pedersen (1955), Report on an experiment in forecasting of cyclone development, *J. Meteorol.*, *12*, 58–67.
Pezza, A. B., and I. Simmonds (2005), The first South Atlantic hurricane: Unprecedented blocking, low shear and climate change, *Geophys. Res. Lett.*, *32*, L15712, doi:10.1029/2005GL023390.
Pfahl, S., and M. Sprenger (2016), On the relationship between extratropical cyclone precipitation and intensity, *Geophys. Res. Lett.*, *43*, 1752–1758, doi:10.1002/2016GL068018.
Pfahl, S., and H. Wernli (2012), Quantifying the relevance of cyclones for precipitation extremes, *J. Clim.*, *25*, 6770–6780.
Pfahl, S., E. Madonna, M. Boettcher, H. Joos, and H. Wernli (2014), Warm conveyor belts in the ERA-Interim data set (1979–2010). Part II: Moisture origin and relevance for precipitation, *J. Clim.*, *27*, 27–40, doi:10.1175/JCLI-D-13-00223.1.
Pfahl, S., P. O'Gorman, and M. S. Singh (2015), Extratropical cyclones in idealized simulations of changed climates, *J. Clim.*, *28*, 9373–9392, doi:10.1175/JCLI-D-14-00816.1.
Pinto, J. G., S. Zacharias, A. H. Fink, G. C. Leckebusch, and U. Ulbrich (2009), Factors contributing to the development of extreme North Atlantic cyclones and their relationship with the NAO, *Clim. Dyn.*, *32*, 711–737.
Pinto, J. G., M. K. Karremann, K. Born, P. M. Della-Marta, and M. Klawa (2012), Loss potentials associated with European windstorms under future climate conditions, *Clim. Res.*, *54*, 1–20.
Pinto, J. G., N. Bellenbaum, M. K. Karremann, and P. M. Della-Marta (2013), Serial clustering of extratropical cyclones over the North Atlantic and Europe under recent and future climate conditions, *J. Geophys. Res. Atmos.*, *118*, 12,476–12,485, doi:10.1002/2013JD020564.
Pinto, J. G., I. Gómara, G. Masato, H. F. Dacre, T. Woollings, and R. Caballero (2014), Large-scale dynamics associated with clustering of extratropical cyclones, *J. Geophys. Res. Atmos.*, *119*, 13,704–13,719, doi:10.1002/ 2014JD022305.
Plant, R. S., G. C. Craig, and S. L. Gray (2003), On a threefold classification of extratropical cyclogenesis, *Q. J. R. Meteorol. Soc.*, *129*, 2989–3012.
Polavarapu, S. M., and W. R. Peltier (1990), The structure and nonlinear evolution of synoptic scale cyclones: Life cycle simulations with a cloud-scale model, *J. Atmos. Sci.*, *47*, 2645–2672.
Polvani, L. M., and J. G. Esler (2007), Transport and mixing of chemical air masses in idealized baroclinic life cycles, *J. Geophys. Res.*, *112*, D23102, doi:10.1029/2007JD008555.
Polvani, L. M., D. W. Waugh, G. J. P. Correa, and S.-W. Son (2011), Stratospheric ozone depletion: The main driver of 20th Century atmospheric circulation changes in the Southern Hemisphere, *J. Clim.*, *24*, 795–812.
Posselt, D. J., G. L. Stephens, and M. Miller (2008), Cloudsat — Adding a new dimension to a classical view of extratropical cyclones, *Bull. Amr. Meteorol. Soc.*, *89*(5), 599–609.
Prater, B. E., and J. L. Evans (2002), Sensitivity of modeled tropical cyclone track and structure of Hurricane Irene (1999) to the convective parameterization scheme, *Meteorol. Atmos. Phys.*, *80*, 103–115.
Purich, A., and S.-W. Son (2012), Impact of Antarctic ozone depletion and recovery on Southern Hemisphere precipitation, evaporation, and extreme changes, *J. Clim.*, *25*, 3145–3154.
Ralph, F. M., P. J. Neiman, G. A. Wick, S. I. Gutman, M. D. Dettinger, D. R. Cayan, and A. B. White (2006), Flooding on California's Russian River: Role of atmospheric rivers, *Geophys. Res. Lett.*, *33*, L13801, doi:10.1029/2006GL026689.
Randall, D. A., et al. (2007), *Climate Change 2007: The Physical Basis, Contribution of Working Group I to the Fourth Assessment Report of the Intergovernmental Panel on Climate Change, Chapter 8: Climate Models and Their Evaluation,* edited by S. Solomon et al., Cambridge Univ. Press, Cambridge, U. K., and New York.
Ranson, M., C. Kousky, M. Ruth, L. Jantarasami, A. Crimmins, and L. Tarquinio (2014), Tropical and extratropical cyclone damages under climate change, *Clim. Change*, *127*, 227–241, doi:10.1007/s10584-014-1255-4.
Rasmussen, E. (1979), The polar low as an extratropical CISK disturbance, *Q. J. R. Meteorol. Soc.*, *105*, 531–549.
Rasmussen, E. (1981), An investigation of a polar low with a spiral cloud structure, *J. Atmos. Sci.*, *38*, 1785–1792.
Rasmussen, E., and J. Turner (Eds.) (2003), *Polar Lows: Mesoscale Weather Systems in the Polar Regions*, 612 pp., Cambridge Univ. Press, Cambridge, U. K.
Raveh-Rubin, S., and H. Wernli (2015), Large-scale wind and precipitation extremes in the Mediterranean: A climatological analysis for 1979–2012, *Q. J. R. Meteorol. Soc.*, *141*, 2404–2417, doi:10.1002/qj.2531.
Reed, R. J. (1979), Cyclogenesis in polar air streams, *Mon. Weather Rev.*, *107*, 38–52.
Reed, R. J., and W. Blier (1986a), A case study of comma cloud development in the eastern Pacific, *Mon. Weather Rev.*, *114*, 1681–1695.
Reed, R. J., and W. Blier (1986b), A further study of comma cloud development in the eastern Pacific, *Mon. Weather Rev.*, *114*, 1696–1708.
Reed., R. J., and C. N. Duncan (1987), Baroclinic instability as a mechanism for the serial development of polar lows: A case study, *Tellus A*, *39A*(4), 376–384, doi:10.1111/j.1600-0870.1987.tb00314.x.

Reed, R. J., G. A. Grell, and Y.-H. Kuo (1993), The ERICA IOP 5 storm. Part II: Sensitivity tests and further diagnosis based on model output, *Mon. Weather Rev.*, *121*, 1595–1612.
Rivals, H., J.-P. Cammas, and I. A. Renfrew (1998), Secondary cyclogenesis: The initiation phase of a frontal wave observed over the eastern Atlantic, *Q. J. R. Meteorol. Soc.*, *124*, 243–267.
Rivière, G., P. Arbogast, and A. Joly (2015), Eddy kinetic energy redistribution within windstorms Klaus and Friedhelm, *Q. J. R. Meteorol. Soc.*, *141*, 925–938, doi:10.1002/qj.2412.
Roberts, J. F., A. J. Champion, L. C. Dawkins, K. I. Hodges, L. C. Shaffrey, D. B. Stephenson, M. A. Stringer, H. E. Thornton, and B. D. Youngman (2014), The XWS open access catalogue of extreme European windstorms from 1979 to 2012, *Nat. Hazards Earth Syst. Sci.*, *14*, 2487–2501, doi:10.5194/nhess-14-2487-2014.
Roebber, P. J. (1984), Statistical analysis and updated climatology of explosive cyclones, *Mon. Weather Rev.*, *112*, 1577–1589.
Romero, R. (2008), A method for quantifying the impacts and interactions of potential-vorticity anomalies in extratropical cyclones, *Q. J. R. Meteorol. Soc.*, *134*, 385–402, doi:10.1002/qj.219.
Rossow, W. B., and R. A. Schiffer (2001), International Satellite Climatology Project (ISCCP) cloud data products, *Bull. Am. Meteorol. Soc.*, *72*, 2–20.
Rudeva, I., and I. Simmonds (2015), Variability and trends of global atmospheric frontal activity and links with large-scale modes of variability, *J. Clim.*, *28*, 3311–3330, doi:10.1175/JCLI-D-14-00458.1.
Sanders, F. (1987), Skill of NMC operational dynamical models in prediction of explosive cyclogenesis, *Weather Forecasting*, *2*, 322–336.
Sanders, F., and J. R. Gyakum (1980), Synoptic-dynamic climatology of the "bomb", *Mon. Weather Rev.*, *108*, 1589–1606.
Sawyer, J. S. (1950), Formation of secondary depressions in relation to the thickness pattern, *Meteorol. Mag.*, *79*, 1–5.
Schemm, S., and M. Sprenger (2015), Frontal-wave cyclogenesis in the North Atlantic—A climatological characterisation, *Q. J. R. Meteorol. Soc.*, *141*, 2989–3005, doi:10.1002/qj.2584.
Schemm, S., and H. Wernli (2014), The linkage between the warm and cold conveyor belts in an idealized extratropical cyclone, *J. Atmos. Sci.*, 1443–1459, doi:10.1175/JAS-D-13-0177.1.
Schemm, S., H. Wernli, and L. Papritz (2013), Warm conveyor belts in idealized moist baroclinic wave simulations, *J. Atmos. Sci.*, *70*, 627–652.
Schoof, J. T., and S. C. Pryor (2014), Assessing the fidelity of AOGCM-simulated relationships between large-scale modes of climate variability and wind speeds, *J. Geophys. Res. Atmos.*, *119*, 9719–9734, doi:10.1002/2014JD021601.
Schultz, D. M. (2001), Reexamining the cold conveyor belt, *Mon. Weather Rev.*, *129*, 2205–2225.
Schultz, D. M., and G. Vaughan (2011), Occluded fronts and the occlusion process: A fresh look at conventional wisdom, *Bull. Am. Meteorol. Soc.*, *92*, 443–466, doi:10.1175/2010BAMS3057.1.
Schultz, D. M., D. Keyser, and L. F. Bosart (1998), The effect of large-scale flow on low-level frontal structure and evolution in midlatitude cyclones, *Mon. Weather Rev.*, *126*, 1767–1791.
Screen, J. A., and I. Simmonds (2013), Exploring links between Arctic amplification and mid-latitude weather, *Geophys. Res. Lett.*, *40*, 959–964, doi:10.1002/grl.50174.
Seiler, C., and F. W. Zwiers (2015), How well do CMIP5 climate models reproduce explosive cyclones in the extra tropics of the Northern Hemisphere, *Clim. Dyn.*, *46*, 1241–1256, doi:10.1007/s00382-015-2642-x.
Serezze, M. C. (1995), Climatological aspects of cyclone development and decay in the Arctic, *Atmos. Ocean*, *33*, 1–23.
Shaffrey, L. C., et al. (2009), U.K.-HiGEM: The new U.K. high-resolution global environment model—Model description and basic evaluation, *J. Clim.*, *22*, 1861–1896.
Shapiro, M. A., and D. Keyser (1990), Fronts, jet streams, and the tropopause, in *Extratropical Cyclones, The Erik Palmén Memorial Volume*, edited by M. A. Shapiro and D. Keyser, pp. 167–191, Am. Meteorol. Soc., Boston, Mass.
Shutts, G. J. (1990), Dynamical aspects of the October storm, 1987: A study of a successful fine-mesh simulation, *Q. J. R. Meteorol. Soc.*, *116*, 1315–1347.
Simmonds, I., K. Keay, and E.-P. Lim (2003), Synoptic activity in the seas around Antarctica, *Mon. Weather Rev.*, *131*, 272–288.
Simmons, A. J., and B. J. Hoskins (1980), Barotropic influences on the growth and decay of nonlinear baroclinic waves, *J. Atmos. Sci.*, *37*, 1679–1684.
Sinclair, M. R. (1997), Objective identification of cyclones and their circulation intensity and climatology, *Weather Forecasting*, *12*, 595–612.
Sinclair, M. R. (2002), Extratropical transition of southwest Pacific tropical cyclones. Part I: Climatology and mean structure changes, *Mon. Weather Rev.*, *130*, 590–609.
Sinclair, M. R., and M. J. Revell (2000), Classification and composite diagnosis of extratropical cyclogenesis events in the Southwest Pacific, *Mon. Weather Rev.*, *128*, 1089–1105.
Sinclair, V. A., S. L. Gray, and S. E. Belcher (2008), Boundary layer ventilation by baroclinic lifecycles, *Q. J. R. Meteorol. Soc.*, *134*, 1409–1424.
Sodemann, H., and A. Stohl (2013), Moisture origin and meridional transport in atmospheric rivers and their association with multiple cyclones, *Mon. Weather Rev.*, *141*, 2850–2868.
Son, S.-W., L. M. Polvani, D. W. Waugh, H. Akiyoshi, R. Garcia, D. Kinnison, S. Pawson, E. Rozanov, T. G. Shepherd, and K. Shibata (2008), The impact of stratospheric ozone recovery on the Southern Hemisphere westerly jet, *Science*, *320*(5882), 1486–1489, doi:10.1126/science.1155939.
Speer, M. S., P. Wiles, and A. Pepler (2009), Low pressure systems off the New South Wales coast and associated hazardous weather: Establishment of a database, *Aust. Meteorol. Ocean J.*, *58*, 29–39.
Stoner, A. M. K., K. Hayhoe, and D. J. Wuebbles (2009), Assessing general circulation model simulations of atmospheric teleconnection patterns, *J. Clim.*, *22*, 4348–4372, doi:10.1175/2009JCLI2577.1.
Strachan, J., P. L. Vidale, K. Hodges, M. Roberts, and M.-E. Demory (2013), Dreary state of precipitation in global models, *J. Clim.*, *26*, 133–152, doi:10.1175/JCLI-D-12-00012.1.
Studholme, J., K. I. Hodges, and C. M. Brierley (2015), Objective determination of the extratropical transition of tropical cyclones in the Northern Hemisphere, *Tellus A*, *67*, 24474, doi:10.3402/tellusa.v67.24474.
Sun, Y., S. Solomon, A. Dai, and R. W. Portmann (2006), How often does it rain?, *J. Clim.*, *19*, 916–934.
Terpstra, A., T. Spengler, and R. Moore (2015), Idealised simulations of polar low development in an Arctic moist-baroclinic environment, *Q. J. R. Meteorol. Soc.*, *141*, 1987–1996, doi:10.1002/qj.2507.
Terpstra, A., C. Michel, and T. Spengler (2016), Forward and reverse shear environments during polar low genesis over the Northeast Atlantic, *Mon. Weather Rev.*, *144*, 1341–1354, doi:10.1175/MWR-D-15-0314.1.
Thorncroft, C. D., and B. J. Hoskins (1990), Frontal cyclogenesis, *J. Atmos. Sci.*, *47*, 2317–2336.
Thorncroft, C. D., B. J. Hoskins, and M. E. McIntyre (1993), Two paradigms of baroclinic-wave life-cycle behaviour, *Q. J. R. Meteorol. Soc.*, *119*, 17–55.

Trenberth, K. E., and J. Fasullo (2010), Simulation of present day and 21st century energy budgets of the Southern Oceans, *J. Clim.*, *23*, 440–454.
Trigo, I. F., T. D. Davies, and G. R. Bigg (1999), Objective climatology of cyclones in the Mediterranean region, *J. Clim.*, *12*(6), 1685–1696, doi:10.1175/1520-0442(1999)012<1685:OCOCIT>2.0.CO;2.
Troup, A. J., and N. A. Streten (1972), Satellite-observed Southern Hemisphere cloud vortices in relation to conventional observations, *J. Appl. Meteorol.*, *11*, 909–917.
Uccellini, L. W., P. J. Kocin, and J. M. Sienkiewicz (1999), Advances in forecasting extratropical cyclogenesis at the National Meteorological Centre, in *The Life Cycles Of Extratropical Cyclones*, edited by M. Shapiro and S. Grønås, pp. 317–336, Am. Meteorol. Soc., Boston, Mass.
Ulbrich, U., A. H. Fink, M. Klawa, and J. G. Pinto (2001), Three extreme storms over Europe in December 1999, *Weather*, *56*, 70–80.
Ulbrich, U., J. G. Pinto, H. Kupfer, G. C. Leckebusch, T. Spangehl, and M. Reyers (2008), Changing Northern Hemisphere storm tracks in an ensemble of IPCC climate change simulations, *J. Clim.*, *21*, 1669–1679.
Ulbrich, U., G. C. Leckebusch, and J. G. Pinto (2009), Extra-tropical cyclones in the present and future climate: A review, *Theor. Appl. Climatol.*, *96*, 117–131.
Vautard, R. (1990), Multiple weather regimes over the North Atlantic: Analysis of precursors and successors, *Mon. Weather Rev.*, *118*, 2056–2081.
Waliser, D. E., and M. Moncrieff (2007), Year of tropical convection—Joint WCRP-THORPEX activity to address the challenge of tropical convection, *WCRP GEWEX News*, *17*(2), 8.
Wang, C.-C., and J. C. Rogers (2001), A composite study of explosive cyclogenesis in different sectors of the North Atlantic. Part I: Cyclone structure and evolution, *Mon. Weather Rev.*, *129*, 1481–1499.
Wernli, H. (1997), A Lagrangian-based analysis of extratropical cyclones. II: A detailed case-study, *Q. J. R. Meteorol. Soc.*, *123*, 1677–1706.
Wernli, H., and H. C. Davies (1997), A Lagrangian-based analysis of extratropical cyclones. I: The method and some applications, *Q. J. R. Meteorol. Soc.*, *123*, 467–489.
Wernli, H., and M. Sprenger (2007), Identification and ERA-15 climatology of potential vorticity streamers and cutoffs near the extratropical tropopause, *J. Atmos. Sci.*, *64*, 1569–1586.
Willison, J., W. A. Robinson, and G. M. Lackmann (2013), The importance of resolving mesoscale latent heating in the North Atlantic storm track, *J. Atmos. Sci.*, *70*, 2234–2250, doi:10.1175/JAS-D-12-0226.1.
Woollings, T., B. Hoskins, M. Blackburn, D. Hassell, and K. Hodges (2010), Storm track sensitivity to sea surface temperature resolution in a regional atmosphere model, *Clim. Dyn.*, *35*, 341–353, doi:10.1007/s00382-009-0554-3.
Woollings, T., J. M. Gregory, J. G. Pinto, M. Reyers, and D. J. Brayshaw (2012), Response of the North Atlantic storm track to climate change shaped by ocean-atmosphere coupling, *Nat. Geosci.*, *5*, 313–317.
Yanase, W., and H. Niino (2005), Effects of baroclinicity on the cloud pattern and structure of polar lows: A high-resolution numerical experiment, *Geophys. Res. Lett.*, *32*, L02806, doi:10.1029/2004GL020469.
Yanase, W., and H. Niino (2007), Dependence of polar low development on baroclinicity and physical processes: An idealized high-resolution numerical experiment, *J. Atmos. Sci.*, *64*, 3044–3067, doi:10.1175/JAS4001.1.
Yanase, W., and H. Niino (2015), Idealized numerical experiments on cyclone development in the tropical, subtropical and extratropical environments, *J. Atmos. Sci.*, *72*, 3699–3714, doi:10.1175/JAS-D-15-0051.1.
Yanase, W., H. Niino, K. Hodges, and N. Kitabatake (2014), Parameter spaces of environmental fields responsible for cyclone development from tropics to extratropics, *J. Clim.*, *27*, 652–671, doi:10.1175/JCLI-D-13-00153.1.
Yanase, W., H. Niino, S.-I. I. Watanabe, K. Hodges, M. Zahn, T. Spengler, and I. A. Gurvich (2016), Climatology of polar lows over the Sea of Japan using the JRA-55 reanalysis, *J. Clim.*, *29*, 419–437, doi:10.1175/JCLI-D-15-0291.1.
Yin, J. H. (2005), A consistent poleward shift of the storm tracks in simulations of 21st century climate, *Geophys. Res. Lett.*, *32*, L18701, doi:10.1029/2005GL023684.
Young, M. V. (1993), Cyclogenesis: Interpretation of satellite and radar images for the forecaster, *Tech. Rep.* 73, Forecasting Research Division, United Kingdom Meteorological Office. [Available from https://digital.nmla.metoffice.gov.uk/file/sdb%3AdigitalFile%7C27f6b1fe-8d1e-4e25-b83c-c356877e00c9/.]
Young, M. V. (1996), Depressions in mid latitudes, in *Images in Weather Forecasting*, edited by M. J. Bader et al., Cambridge Univ. Press, Cambridge, U. K.
Zahn, M., and H. von Storch (2008), A long-term climatology of North Atlantic polar lows, *Geophys. Res. Lett.*, *35*, L22702, doi:10.1029/2008GL035769.
Zappa, G., L. C. Shaffrey, and K. I. Hodges (2013), The ability of CMIP5 models to simulate North Atlantic extratropical cyclones, *J. Clim.*, *26*, 5379–5396, doi:10.1175/JCLI-D-12-00501.1.
Zappa, G., L. Shaffrey, and K. Hodges (2014), Can polar lows be objectively identified and tracked in the ECMWF operational analysis and the ERA-Onterim reanalysis?, *Mon. Weather Rev.*, *142*(8), 2596–2608, doi:10.1175/MWR-D-14-00064.1.
Zhang, X., J. E. Walsh, J. Zhang, U. S. Bhatt, and M. Ikeda (2004), Climatology and internal variability of Arctic cyclone activity: 1948–2002, *J. Clim.*, *15*, 2300–2317.
Zillman, J. W., and P. G. Price (1972), On the thermal structure of mature Southern Ocean cyclones, *Aust. Meteorol. Mag.*, *20*, 34–48.
Zolina, O., and S. K. Gulev (2003), Synoptic variability of ocean-atmosphere turbulent fluxes associated with atmospheric cyclones, *J. Clim.*, *16*, 2717–2734.